Article

Bill It Right: Evaluating Public Charging Station Usage Behavior under the Presence of Different Pricing Policies

Markus Fischer [1,*] , Wibke Michalk [2] , Cornelius Hardt [3] and Klaus Bogenberger [1]

1 Chair of Traffic Engineering and Control, Technical University of Munich, 80333 Munich, Germany; klaus.bogenberger@tum.de
2 Campus Chiemgau, Rosenheim Technical University of Applied Sciences, 83278 Traunstein, Germany; wibke.michalk@th-rosenheim.de
3 Fraunhofer Institute for Material Flow and Logistics IML, 83209 Prien am Chiemsee, Germany; cornelius.hardt@iml.fraunhofer.de
* Correspondence: markus.dieter.fischer@tum.de

Abstract: This study investigates for the first time how public charging infrastructure usage differs under the presence of diverse pricing models. About 3 million charging events from different European countries were classified according to five different pricing models (cost-free, flat-rate, time-based, energy-based, and mixed) and evaluated using various performance indicators such as connection duration; transferred energy volumes; average power; achievable revenue; and the share of charging and idle time for AC, DC, and HPC charging infrastructure. The study results show that the performance indicators differed for the classified pricing models. In addition to the quantitative comparison of the performance indicators, a Kruskal–Wallis one-way analysis of variance and a pairwise comparison using the Mann–Whitney-U test were used to show that the data distributions of the defined pricing models were statistically significantly different. The results are discussed from various perspectives on the efficient design of public charging infrastructure. The results show that time-based pricing models can improve the availability of public charging infrastructure, as the connection duration per charging event can be roughly halved compared to other pricing models. Flat-rate pricing models and AC charging infrastructure can support the temporal shift of charging events, such as shifting demand peaks, as charging events usually have several hours of idle time per charging process. By quantifying various performance indicators for different charging technologies and pricing models, the study is relevant for stakeholders involved in the development and operation of public charging infrastructure.

Keywords: electric vehicles; usage behavior of charging infrastructure; charging tariffs; pricing models; pricing of PEV charging; pricing policy; pricing mechanisms

1. Introduction

The transport sector is a central source of greenhouse gas (GHG) emissions in modern economies [1,2]. For instance, the transport sector is responsible for around 25 and 28% of total GHG emissions in Europe and the USA, respectively, and road transport accounts for the largest share of emissions at around 3/4 [3–6]. In addition to a modal shift, the electrification of vehicles is a crucial field of action for reducing GHG emissions in the transport sector.

In 2023, 14.2 million new plug-in electric vehicles (PEVs) were registered worldwide, which corresponds to an increase of 35% compared to the previous year with 10.5 million PEVs [7,8]. Various studies have indicated that the acceptance and spread of PEVs can be supported by the development of public charging infrastructure (CI) [9–11]. In this context, understanding usage behavior is the basis for optimizing the existing and future public CI. Consequently, the usage behavior of CI has already been investigated in many aspects. Various studies have investigated, for example, the effect of push measures that

include price incentives on mobility behavior. For example, research shows that introducing parking fees or increasing existing fees helps to reduce the use of private vehicles and make alternative modes of transportation more attractive [12–14]. However, charging behavior under the presence of different pricing schemes has yet to be examined in detail. The current state of research and the novel contribution of this study are presented below.

Table 1 shows an overview of relevant investigations into public CI usage behavior. The column *Number of CEs* lists the number of charging events (CEs) at the charging points (CPs) on which the research was based. The column *Period* lists the collection period of the CEs. The subsequent columns *CI-Types*, *Location*, and *Pricing Models* provide thematic insights into the investigations. *CI-Types* indicates whether the study differentiated between types of public CI and different charging technologies. *Location* indicates whether charging infrastructure locations were considered in the investigation, and *Pricing Models* whether the pricing of public CEs was considered in the study.

Table 1. Overview related literature.

Authors	Number of CEs	Country	Period	CI-Types	Location	Pricing Models
Sun et al. (2015) [15]	61,000	Japan	2011–2013	-	-	-
Sun et al. (2015) [16]	5000	Japan	2011–2013	-	-	✓
van den Hoed et al. (2013) [17]	135,000	Netherlands	2012–2013	-	-	-
Motoaki and Shirk (2017) [18]	8000	USA	2013	-	-	✓
Morrissey et al. (2016) [19]	40,000	Ireland	2012–2015	✓	✓	-
Wolbertus et al. (2016) [20]	1.6 m	Netherlands	2014–2015	-	-	-
Wolbertus et al. (2017) [21]	1.3 m	Netherlands	2016	-	-	-
van der Kam et al. (2020) [22]	1 m	Netherlands	2016–2018	-	-	-
Wolbertus et al. (2021) [23]	1.6 m	Netherlands	2017–2018	✓	-	-
Fischer et al. (2022) [24]	300,000	Germany	2020	✓	✓	-
Hecht et al. (2020) [25]	-	Germany	2019–2020	-	✓	-
Friese et al. (2021) [26]	-	Germany	2021	✓	✓	-
Mortimer et al. (2022) [27]	1.8 m	Germany	-	-	✓	-
Hecht et al. (2022) [28]	9 m	Germany	2019–2021	✓	-	-
Jonas et al. (2023) [29]	2.3 m	Canada	2018–2019	✓	✓	-
Borlaug et al. (2023) [30]	1.5 m	USA	2019–2022	✓	✓	-
Mahlberg et al. (2023) [31]	4000	USA	2022	✓	-	-

In [15,16], the charging behavior of private and commercial PEVs was investigated, with a focus on AC CEs in the former, and DC CEs in the latter. The data of about 500 battery electric vehicles (BEVs) with a maximum range of up to 180 km collected in Japan from 2011 to 2013 served as the basis for the study. For AC CEs, the study examined whether the CE started immediately after the arrival of the last trip or whether there was a delay in between. A delay was assumed if the CE had not started within 30 min after arrival. The analysis of AC CEs showed that there was a delay in 20% of the CEs of commercial BEVs and in 55% of private BEVs. According to [15], the high share of delay in private BEVs resulted from the CEs at private charge points (CPs). The users waited until a favorable electricity tariff was in effect between 11 p.m. and 7 a.m. Part of the DC CI was cost-free, and part was paid. The results of the study showed no relevant difference between the cost-free and paid use of DC CI in terms of the state-of-charge (SOC) at the start of the CE and, thus, in terms of the energy quantities transferred.

In [18], the usage behavior at DC CI was investigated for two different pricing models. For this purpose, the connection duration and the transferred energy quantity were compared for a cost-free and flat-rate charging of USD 5 per CE. Approximately 6000 DC CEs from private Nissan Leaf owners with a nominal DC power of 50 kW were used as the database. The results showed that CEs with flat-rate pricing models had lower energy volumes per minute and longer connection times than cost-free CEs.

In [17,20,21], the usage behavior at public CI was investigated using public CE data from different Dutch cities collected from 2012 to 2016. These studies quantified characteris-

tic values for connection duration, transferred energy quantities, and the share of idle time for individual charging locations. Comparable research was presented in [19,24–26,28] for public CI from the European countries of Ireland, Northern Ireland, and Germany from 2012 to 2021. These studies thus form a reasonable basis for comparing usage behavior. Tariffs were not investigated in these studies.

In [22,23,27], different planning approaches for scaling public CI were compared. The studies were based on an extensive dataset of over one million CEs. In [22], possible roll-out strategies for policymakers were structured using a decision tree. Accordingly, the recommendations for action were mainly based on the share of charging and idle time. In [23], different approaches for the roll-out of public CI in cities were investigated with the installation of isolated AC charging stations (CSs) and several AC CSs at one location as charging hubs and DC CI. In [27], a competitive and cooperative planning approach for the roll-out of public CI were compared. The competitive approach resembled a market-based approach, in which private companies build charging sites primarily in the most attractive locations. In contrast, the cooperative approach was more like a policy-driven approach, where new CSs are primarily developed at locations with a low density of existing CSs, to improve the overall coverage of public CI. The study was based on data from publicly available websites. Since this dataset only contained information about the temporal occupancy of public CI, relevant aspects such as the transmitted energy quantity or tariffs were not considered in the evaluation.

In [29], patterns were identified in the charging behavior of PEVs at private and public charging points. The study was based on data from around 2.3 million CEs at over 7000 public and private CSs in Canada. The results indicated an "EV duck curve" with a peak in demand in the evening hours due to private CEs. Due to the loss of solar power during this time, there is a risk that the energy demand will be covered by fossil fuels, thus worsening the carbon footprint of PEVs. Dynamic pricing strategies were mentioned as a possible solution to shift the demand for power to periods with electricity from renewable energy sources. In [30], the usage behavior of public CI in the USA and the influence of various factors were examined using regression analyses. The study differentiated between AC and DC CSs and between free and paid CEs. The results showed that the proportion of idle connection time at AC CSs was much higher (30 to 76%) than the proportion at DC CSs (5 to 11%). The comparison of free and paid CEs showed that offering cost-free CEs can improve the utilization of AC CI in particular. This study also pointed to the need for future studies in which the usage behavior of public CI is examined for different pricing models. In [31], the activity of users during public CEs was observed using cameras. In total, the activities during 4000 CEs at 16 DC and HPC CSs with 50, 150, and 350 kW nominal power were evaluated in the period from May to July 2022 at two charging locations in America. It should be noted that only the camera data on user activity were evaluated. Data on the actual CEs, such as the amount of energy transferred, were not recorded. The driver's activity during the CEs was divided into six categories (wait in vehicles, travels to stores, travels to stores and waits in vehicles, walks pet, unknown, and left the premises), with each activity affecting the average time spent at the CSs. For example, the connection time for users who left the charging location was 30 to 60 min longer than for users who waited in their vehicles.

In summary, the previous studies primarily investigated the user behavior of public CI on the basis of various data sources from single countries. In some studies, user behavior was examined separately for individual CI and location types. However, pricing models were not considered. In [16,18], CE pricing was considered as a secondary aspect for DC CEs, but only whether pricing occurred or whether CEs were free. Furthermore, since these studies were conducted on PEV-based datasets, the number of CEs was comparatively small. In contrast to previous studies, the study at hand provides a detailed evaluation of different pricing models separately for AC, DC, and HPC CI. Based on an extensive dataset of real public CEs from different European countries, different pricing models are identified and classified for this purpose. Furthermore, the charging locations are classified

and analyzed into different location types and analyzed. Thus, the present study covers all research areas listed in Table 1.

2. Materials and Methods

2.1. Dataset

This study is based on a dataset containing more than 3.1 million charge detail records (CDRs) from public CEs. Such records are the data footprint of CEs and are utilized, among other things, in the billing process. Table 2 lists the data points included in these records. Each record contains an *EVSEID* ("Electric Vehicle Supply Equipment Identification") as unique identifier for the utilized CP, the *transaction_begin* and *transaction_end* that allow calculating the connection duration, the amount of transferred energy, the *price* billed to the customer, the *tariff* applied as a unique code, as well as the *tariff_text*, a textual description of this tariff. The dataset contains a total of over 4000 different tariffs. The data points *latitude* and *longitude* describe the location of the CP, while *charging_type* and *power* indicate the charging technology and the nominal power of the CP. Here, a DC CP with a power of 150 kW or more is considered as HPC [32]. Various logical checks were performed to filter out erroneous and illogical CEs. For example, CEs with no transferred energy or CEs with more than 150 kWh transferred were excluded, as in the record period there were no PEVs in the market able to accumulate so much energy. CEs with a connection duration below 5 s or above 48 h were excluded, since these records have a high probability of error. Further exclusions were made of incomplete records. The remaining 2.6 million CEs were the basis for subsequent analyses.

Table 2. Description of the dataset.

Variable Name	Description	Unit
EVSEID	Identification of the charging point	Unique ID
transaction_begin	Start time of the connection	dd:mm:yyyy hh:mm:ss
transaction_end	End time of the connection	dd:mm:yyyy hh:mm:ss
kWh	Transmitted energy during the connection	kWh
price	Accounted price for the charging event	Euro
tariff	Tariff code	Unique ID
tariff_text	Description text for the tariff code	String
latitude and longitude	Longitude and latitude to identify the location of the charging station	Geographical coordinates
charging_type	Information whether it is an AC or DC charging point	AC or DC
power	Nominal charging power of the charging point	kW

The dataset for this study is provided by Wirelane, a backend provider for public CI, and includes CEs from 2020 till 2022. Wirelane, as an e-mobility service provider (EMSP), enables PEV users to access various public CI. A charge point operator (CPO) operates the CPs and provides the EMSP with technical and economic access to the CP for its e-mobility users. Access is provided via authorization media that the EMSP provides to the e-mobility user. In addition, a core task of the EMSP is to charge the e-mobility user for the CE [33,34] in accordance with the CPO's terms.

In contrast to the CPO view, the dataset of this study only included the CEs that had been processed via the respective EMSP. Thus, the dataset at hand did not include the entirety of all CEs at single CPs but only those that had been handled by the EMSP. Therefore, the dataset at hand did not allow for a thorough analysis of usage of each individual CP but gave insights into the general usage of CPs based on different tariffs for a multitude of CPs for various CPOs.

Taking the city of Munich as an example, the EMSP-dataset includes about 50% of the CEs from 2020 to 2022 that were made at the public CSs of Stadtwerke München (SWM), Munich's largest CPO. For reference, the SWM's CPO dataset was used in [24,35]. However, unlike CPO datasets, the EMSP dataset includes greater geographic coverage of charging locations. Statements such as the utilization or the profitability of individual CSs or charging

locations cannot be calculated based on the EMSP dataset, since only the EMSP's share of CEs is included. Figure A1 in the Appendix A compares the relative data distributions from the EMSP and CPO datasets for Munich. The EMSP dataset comprises 800,000 AC-CEs and 11,000 DC-CEs that took place in Munich between 2020 and 2022. The CPO dataset, which contains the population of all CEs at the charging locations, comprises 1.7 million AC-CEs and 25,000 DC-CEs for the same period. The distribution of the connection duration and the amount of energy transferred were visualized separately for AC and DC CEs and showed similarities in the data distributions of the EMSP and CPO dataset for Munich.

Figure 1 visualizes the CI locations. The map shows that most CPs are located in Germany and France; 70% of the CPs are located in Germany, while 18% are located in France. The remaining 12% of CPs are spread over 21 other countries. Figure A2 in the Appendix A shows the distribution of CEs by country and their evolution from 2020 through 2022. Accordingly, about 88% of CEs were made in Germany and 11% in France, and the remainder were distributed among other countries. It should be noted that the share of CEs made in Germany increased over the years 2020, 2021, and 2022 from 60 to 87 and 99%. In the same period, the share of CEs in France decreased from 39 to 12 and below 1%. Since the dataset mainly contains CEs from Germany and France, additional KPIs for these two countries have been included in the Appendix A. Tables A1–A3 list KPIs for CI separately by charging technology for France and Germany. However, as the analyzed dataset does not cover any customer-specific information or any information on the used vehicles, no further analysis was carried out in the work at hand. This is elaborated in more detail in Section 5.
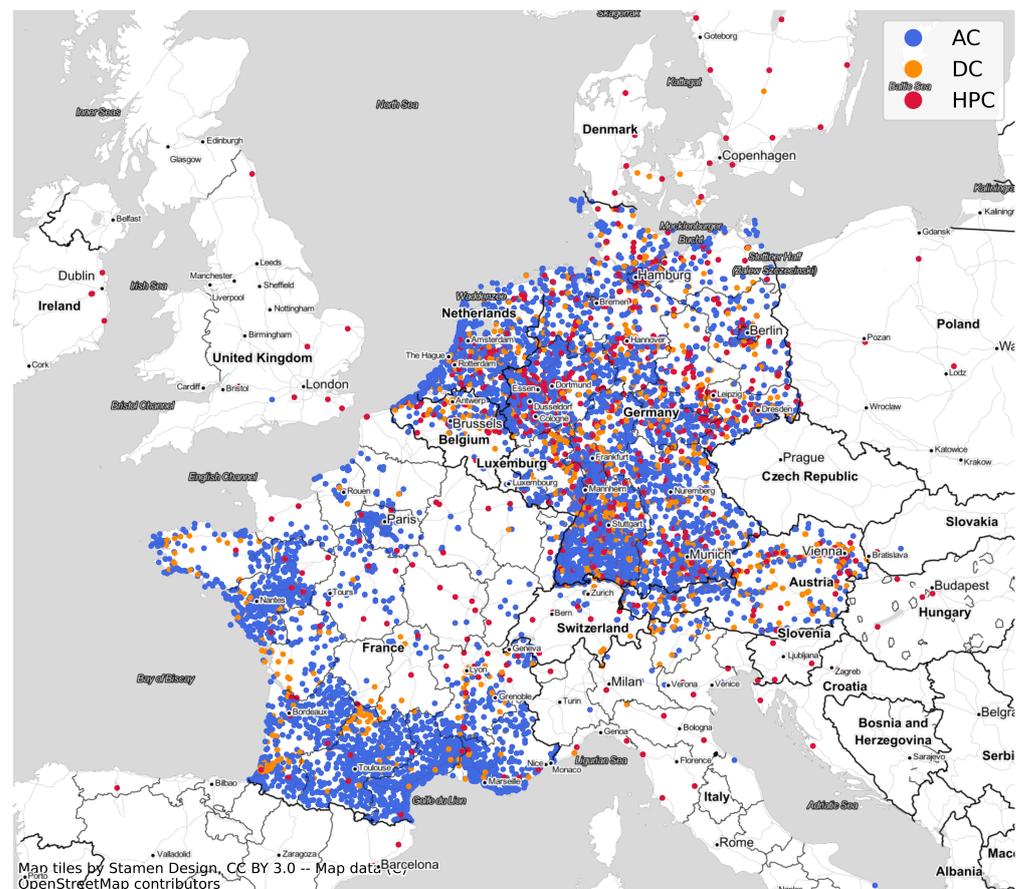

Figure 1. Location of the charging points in the dataset.

For a more differentiated assessment of the spatial distribution of CI, the charging locations were divided into four location types: highway, urban, intermediate, and rural. The location type highway was defined in dependence of the distance to the next highway

and the other categories in dependence of the population density [36,37]. The thresholds used for highway location type were 500, 1000, and 2000 m. The results show that the majority of HPC CIs had the highway location type. In contrast, AC and DC CI was preferably located in urban or intermediate areas. Table A4 and Figure A3 in the Appendix A show the results and the geospatial data used. The location types are used in the following as a basis for further analyses.

Tables 3–5 describe the dataset separately for AC, DC, and HPC CEs and for the years 2020, 2021, and 2022. This differentiated view is intended to enable a more profound understanding of the dataset. The columns *Number of CPs* and *Number of CEs* indicate how many CPs and CEs the dataset contains in the respective year and the column *Power Range* indicates the range of the nominal charging power of the CPs. The last two columns contain key figures for the amount of energy transferred and the connection duration per CEs. All charging technologies showed an increasing *Number of CPs* and *Number of CEs* over time.

Table 3. KPIs of AC charging events from the real-world dataset.

Period	Number of CPs	Number of CEs	Power Range [kW]	Avg./Median Con. Duration [h/CE]	Avg./Median Energy [kWh/CE]
2020	11,700	390,000	3–43	4.9/2.8	16.4/11.2
2021	16,300	790,000	3–43	5.1/3.1	15.7/10.9
2022	18,900	1.1 m	3–43	4.8/3.1	14.9/10.6

Table 4. KPIs of DC charging events from the real-world dataset.

Period	Number of CPs	Number of CEs	Power Range [kW]	Avg./Median Con. Duration [h/CE]	Avg./Median Energy [kWh/CE]
2020	1300	25,000	22–125	0.8/0.5	18.4/14.4
2021	2200	41,000	22–140	0.9/0.6	21.1/17.7
2022	2000	45,000	22–140	1.0/0.7	23.1/19.9

Table 5. KPIs of high-power charging events from the real-world dataset.

Period	Number of CPs	Number of CEs	Power Range [kW]	Avg./Median Con. Duration [h/CE]	Avg./Median Energy [kWh/CE]
2020	260	900	150–320	0.6/0.6	30.3/27.6
2021	2800	26,000	150–400	0.6/0.5	27.1/23.5
2022	4700	76,000	150–400	0.5/0.5	28.8/26.0

For AC CI, about 60% more CPs and about 180% more CEs were recorded in 2022 than in 2020. An interesting aspect emerges when the growth rates of DC and HPC CI are compared. A large increase in DC CPs can be seen from 2020 to 2021, with about a 70% and about 65% increase in DC CEs recorded. From 2021 to 2022, the number of DC CPs in the dataset decreased by about 10%, while the number of DC CEs increased further by about 10%. A different picture in terms of growth rates arises for HPC CI. The relative growth rates were high in both comparison periods. For example, in 2022, more connections were recorded at HPC CPs than at DC CPs, with approximately 76,000 CEs. With the data at hand, strong growth is particularly evident in HPC CI. Since there is a technological proximity between HPC and DC CI and the growth rates of DC CI were stagnant, it is valid to assume that the growth of HPC CI occurred at the expense of DC CI.

Consideration of the nominal power of each CP reveals a *Power Range* for the various charging technologies. Although the range of nominal power is relatively wide, certain power classes are standard. For example, over three-quarters of the surveyed AC, DC, and HPC CPs had a nominal power output of 22, 50, and 300 kW, respectively.

Considering *Connection Duration* and *Transmitted Energy* per CE, differences in the usage patterns of the different charging technologies become apparent. Typically, AC CEs

had an average connection duration of about 5 h and transmitted an average of about 15 kWh. In comparison, DC and HPC CEs lasted only about 0.5 to just under 1 h on average and transferred nearly twice as much energy per CE than AC CEs, i.e., 18 to 30 kWh. Figures A4–A6 provide additional analyses in this context. A comparison of the nominal and average power per charging technology is given in Figure 2. The black dots in the violin plots show the median of the distribution. Here, the average power was calculated by dividing the amount of transmitted energy by the connection duration. The comparison shows that the average power was significantly lower than the nominal power for each charging technology.


(**a**) AC charging events

(**b**) DC charging events

(**c**) High-power charging events
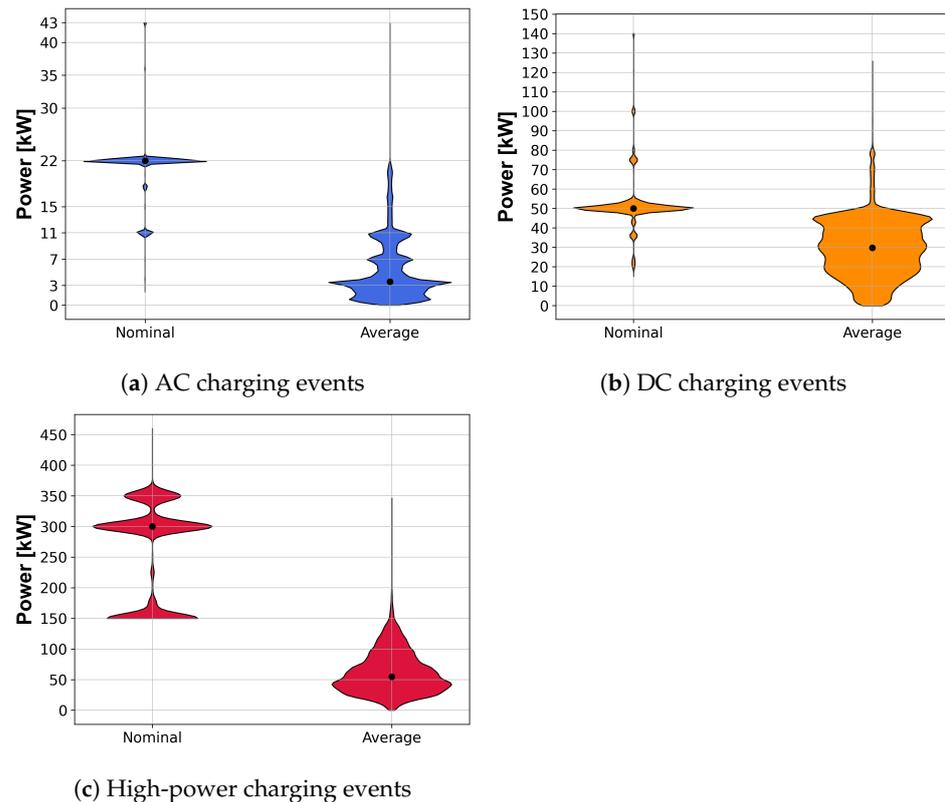
Figure 2. Nominal and average charging power of AC, DC, and high-power charging events.

The median of the average charging power of AC CEs was about 3.6 kW, which is more than 80% lower than the median nominal power of 22 kW. The deviation is about 40% and 80% for DC and HPC CEs, respectively, with 31.2 and 54.6 kW in average power and 50 and 300 kW in nominal power. These significant differences between the possible nominal power of the CP and actual average charging power result from several factors. First, the maximum possible power of PEVs is significantly lower than the possible nominal power of CPs in the case of AC and HPC CEs [35]. Second, the battery management system reduces vehicle charging power when the SOC level increases, to prevent overcharging of the battery cells. Third, differences stemmed from usage behavior at CI. For example, AC CPs tend to be occupied for longer than necessary for the actual CE [21,24]. Tables A6 and A7 additionally list the nominal and average power for different percentile values.

2.2. Classification of Pricing Models

Based on the price composition given in the dataset by the *tariff_code* and description, the underlying pricing model for each CE was classified. In an additional step, the pricing models categorized were logically checked to ensure consistency. Figure 3 shows the classification of the charging events according to the price composition and the price level of the billed CEs.
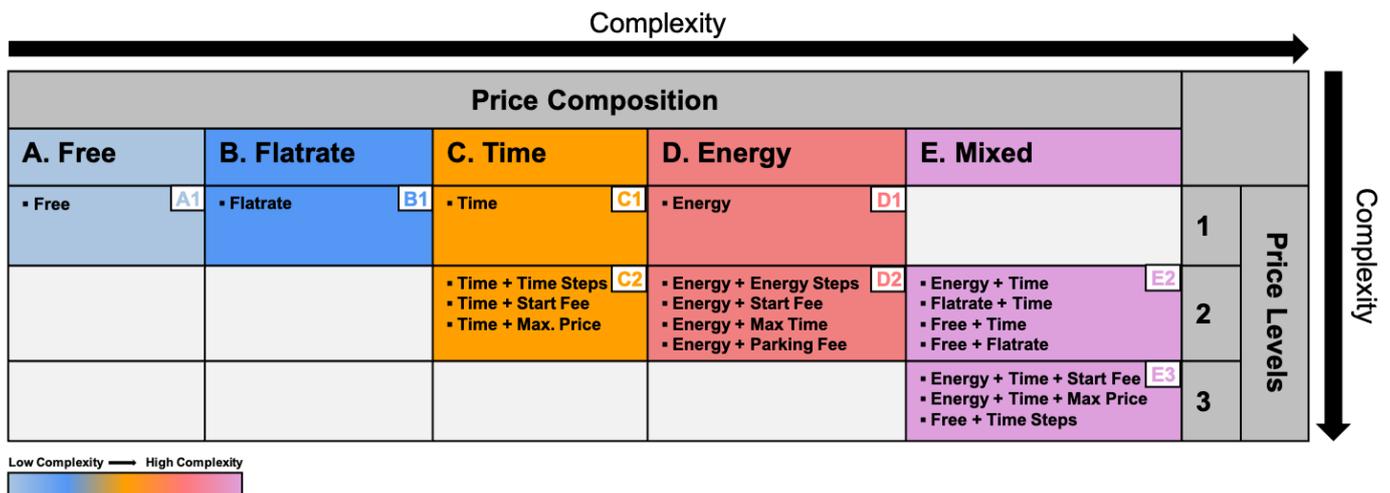
Figure 3. Classification of the charging events according to pricing models.

The price composition indicates which attributes are employed with a specific pricing. Accordingly, four different characteristics were identified in the dataset. In class *A. Free*, there is no billing, and the CE is free of charge. In class *B. Flatrate*, the CE is billed at a flat-rate, regardless of the connection duration to the CP and the amount of energy transferred. In class *C. Time*, the billing is based on the connection duration, and in class *D. Energy*, billing is based on the amount of energy transmitted. Class *E. Mixed* represents a mixed form, in which at least two of the previous classes have been combined; for example, in the form of an energy- and time-based pricing model. The price level indicates how many levels the pricing model has. For example, time-based billing in class *C. Time* may contain different prices for short and long connection durations and thus have two price levels. In the analysis, a distinction could be made between classes and subclasses. For classes, CEs were classified solely based on the general type of tariff. Classes included CEs with the same price composition but different price levels. For subclasses, CEs were additionally classified by price level. As a result, for each of the applicable classes, two subclasses were formed (cp. Figure 4).

Figure 4 shows the share of formed classes and subclasses in the dataset. More than 65% of the CEs were billed using energy-based pricing models of class *D. Energy*. The high share of energy-based pricing models resulted from the fact that most of the CEs took place in Germany, as depicted in Figure A2. Legal regulations concerning the billing of public CPs seen in the dataset are based on the EU Directive 2014/94/EU, on developing alternative fuel infrastructure [38]. The directive was adopted on 22 October 2014 and must be implemented into national law by all EU member states. Among other things, it stipulates minimum requirements concerning the billing at public CI and the transparency thereof. Based on this directive, national legislation in Germany articulates that costs at CI are to be calculated predominantly by consumed energy in kWh, while mixed calculations are not ruled out explicitly.The regulation applies to all public CPs installed after 1 April 2017, with a transition period for older CPs [39,40]. National legislation in France is comparable, but additionally allows for the application of purely time-based tariffs. The transitional period for older CPs is given as well [41]. In the Appendix A, the distribution of classified pricing models for different countries from 2020 to 2022 is shown in Figure A15. The analysis showed that pricing models of class *D. Energy* are predominant in Germany. In comparison, pricing models in other European countries are much more heterogeneous. Thus, this study evaluated the effects of the different national interpretations of the European Directive.
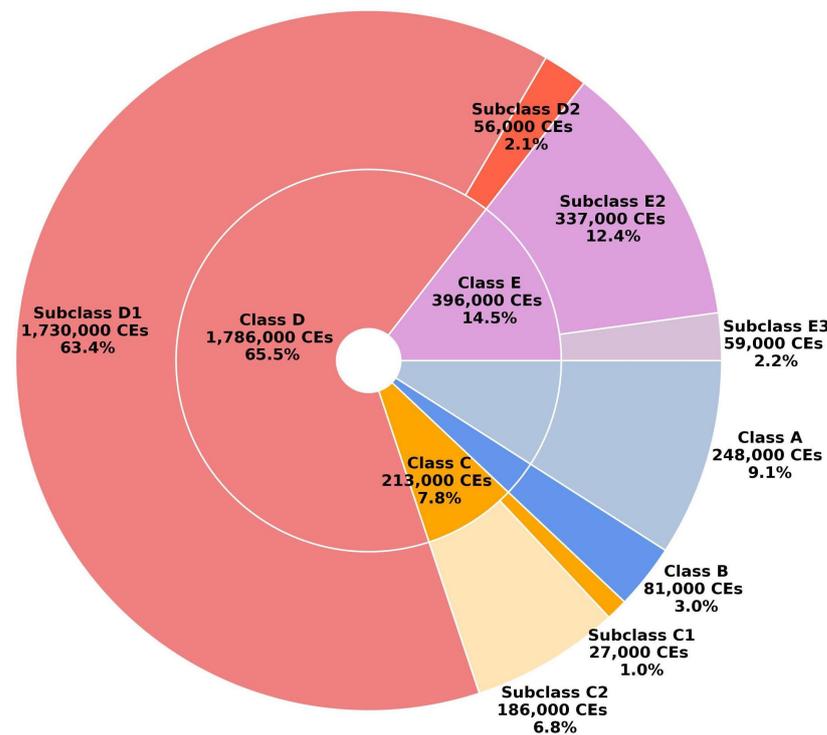
Figure 4. Distribution of the classified pricing models.

The distribution in Figure 4 shows that subclasses with a lower number of price levels have a higher share in most classes. Only in class *C. Time* is the subclass *C2. Time* dominant. This can be explained by the fact that in the case of time-based billing, a second price component is usually included to limit or reduce the maximum billing amount for the e-mobility user.

Figure 5 shows the distribution of classes formed from 2020 to 2022, broken down by AC, DC, and HPC CEs. Over time, a decreasing proportion of cost-free CEs for AC and DC CI can be seen. The results also show an increase in the share of class *D. Energy* in AC and DC CEs. For example, the share of energy-based tariffs increased from ∼45% to ∼75% and from ∼20% to over 60% for AC and DC CEs, respectively, between 2020 and 2022. A more heterogeneous distribution of the classified pricing models can be seen for HPC CEs: In 2020, ∼55% of CEs were accounted for by class *D. Energy* and ∼34% by class *B. Flatrate*. In 2022, the classes *D. Energy*, *E. Mixed* and *C. Time* represented the majority of CEs, with over 90%.

Furthermore, it is striking that cost-free charging did not play a significant role in HPC charging, compared to AC and DC charging. Not even 1% of HPC charging processes were free of charge, which can be explained by the higher investment and operating expenses for HPC CI [28,35]. In comparison, the proportion of cost-free CEs for AC and DC CI was higher than for charging according to flat-rate price models. This difference may be because AC and DC CI were built before HPC CI. The CSs, therefore, partly belonged to the first generation of CI, in which the necessary hardware for custody transfer billing could not be installed. Therefore, fee-based billing was not possible or not desired. The distribution of classes in the individual years is influenced by the countries and their respective legal requirements. For example, in the period under review from 2020 to 2022, the share of CEs occurring in Germany rose from ∼60% to over 99%. Since energy-based pricing models dominate in Germany due to national legislation, the dataset also shows a high share of energy-based pricing models for all charging technologies. A detailed analysis of the distributions by country, class, and period can be found in Figures A2 and A15.

(**a**) AC charging events 2020   (**b**) AC charging events 2021   (**c**) AC charging events 2022

(**d**) DC charging events 2020   (**e**) DC charging events 2021   (**f**) DC charging events 2022

(**g**) High power charging events 2020   (**h**) High power charging events 2021   (**i**) High power charging events 2022
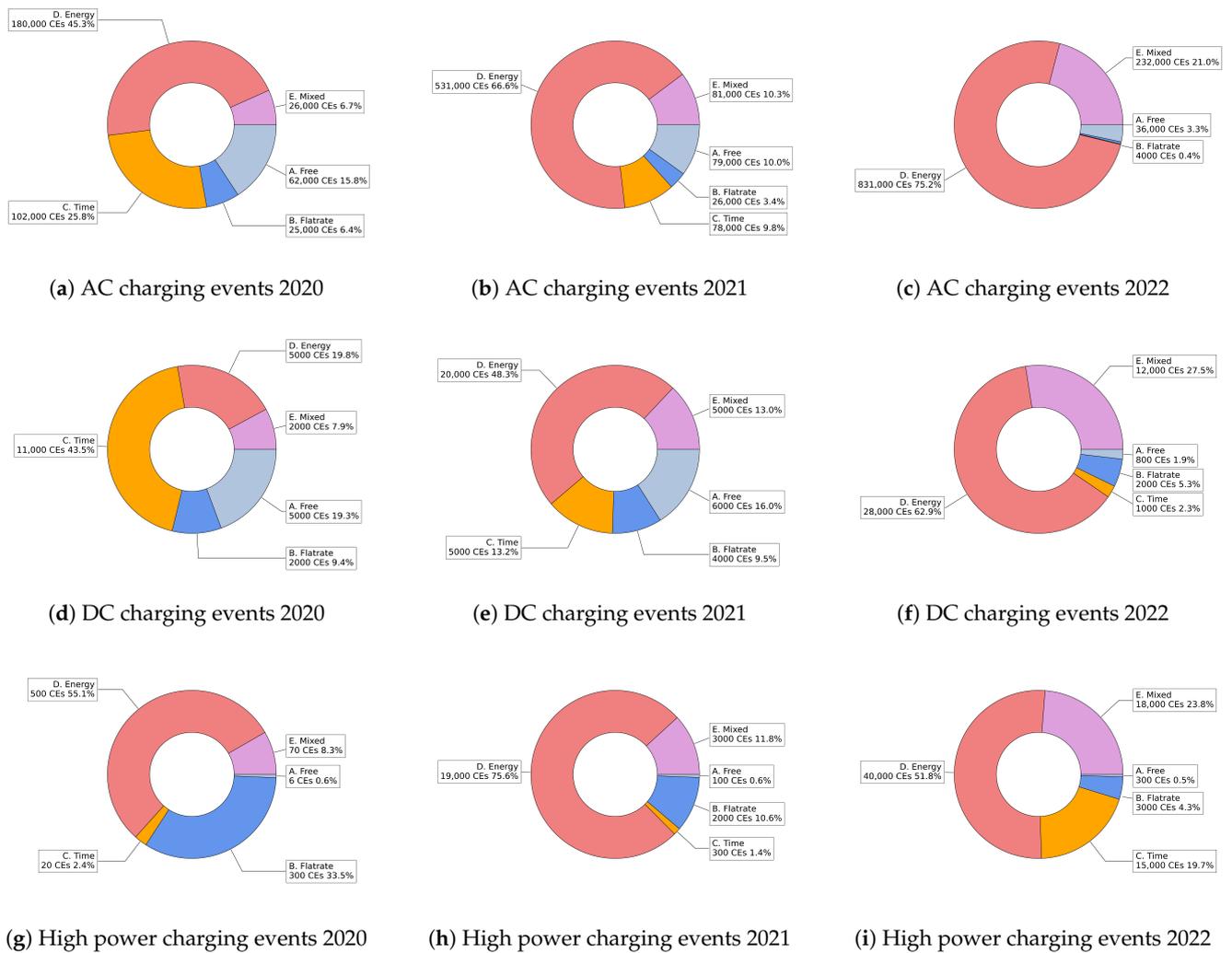
Figure 5. Distribution of the classified pricing models per charging technology and period of time.

2.3. Charging or Idling

This study's main objective is to determine if different usage behaviors of public CI are exhibited when different pricing models are employed. In addition to the connection duration and the amount of energy transferred, the proportion of charging and idle time is an essential performance indicator for evaluating CI efficiency. Idle time describes the proportion of the connection duration for which the PEV is connected to the CP but the actual energy transfer has already been completed. From an efficiency perspective, the proportion of idle time should be minimized to increase the availability of public CI and, thus, the amount of energy that can be transmitted.

Since the dataset does not contain direct information about the charging and idle time-share, these shares were estimated by applying the methodology presented in [24]. Here, different charging areas were defined based on the charging technology. The charging ranges were defined based on the constant current constant voltage CCCV method [18,42,43]. Table A5 lists the parameters employed to create the charging areas. The methodology's basic idea is that each CE can be described by the parameters *duration of the connection* and *amount of energy transferred*. Creating charging areas helps to determine whether the CE is inside or outside the charging areas. If the CE is inside, the CE has no idle time. If the CE is outside the charging area, the charging and idle time can be quantified with the help of the horizontal intersection points of the charging areas.

3. Results

3.1. Usage Behavior

The applied classification of CEs by pricing models allowed investigating differences in usage behavior with respect to the present pricing models, i.e., differences in charging and idling time by tariff. When interpreting the analysis results, the dataset's limitations need to be taken into account: (1) It is not feasible to carry out causal analyses between price models and usage behavior as information is missing; e.g., if tariff choice is based on expected charging behavior or if charging behavior is adapted based on tariff choice. (2) The dataset only contains the subset of CEs at individual locations, which were processed by the EMSP, rather than the total of all CEs at the location. As the authors did not have access to data from CPOs that would allow them to compare charging behavior at different locations (or even for different price models), it was not feasible to generalize the findings in their totality.

The connection duration was the critical parameter for determining the time utilization of the CPs. Figure 6 shows the distribution of connection durations per pricing model, separated by charging technology. No distinction is made between individual price levels or subclasses. The distributions show that there are large differences between connection durations of AC CEs per pricing model. For example, the median connection duration per CE for *B. Flatrate* is 4.9 h, more than twice as high as for *C. Time* with 2.2 h. The highest connection durations are exhibited by AC CEs with pricing models of the classes *D. Energy*, *A. Free*, and *B. Flatrate* with a median of 3.3 h, 3.6 h, and 4.9 h per CE. Although the absolute differences in connection duration are smaller for DC and HPC CEs than for AC CEs, differences in usage behavior can still be observed. An apparent difference under the presence of time-based pricing models of the class *C. Time* is observed: with time-based pricing in place, connection times were shorter on average. Table A8 lists different percentile values of connection durations per class and charging technology.


(**a**) AC charging events

(**b**) DC charging events

(**c**) High-power charging events
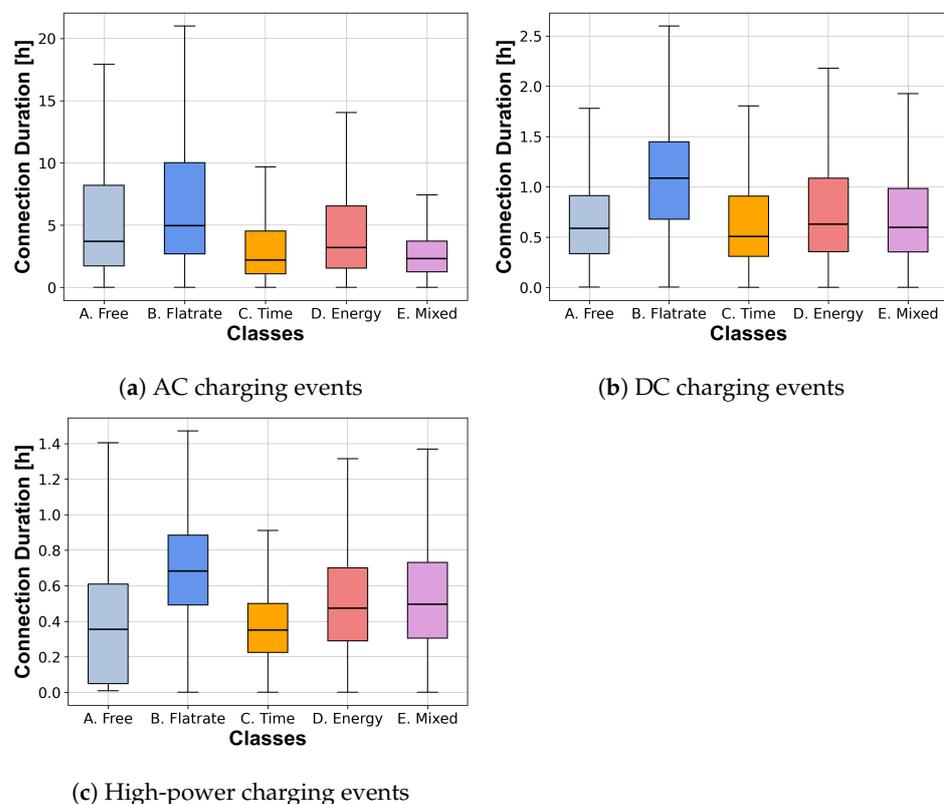
Figure 6. Connection duration per pricing model class of AC, DC, and high-power charging events.

Figure 7 shows the average connection duration by connection start time. For AC CEs, the plots show that for classes *C. Time* and *E. Mixed*, the connection duration for CEs were lower, regardless of connection start time. For CEs starting between 8 a.m. and 6 p.m., average connection durations were about 2.7 h and 2.9 h for classes *C. Time* and *E. Mixed*, which is about 35% to 50% shorter compared to the other classes. For CEs starting between 6 p.m. and midnight, average connection durations were 30% to 38% lower for these classes. As seen in Figure A5, the connection duration of DC and HPC CEs shows less differences with respect to start times compared to AC CEs, the distributions of the classes are also less characteristic in this case.

In addition to the connection duration, the transmitted energy quantities are another critical parameter, since supplying the PEVs with energy is the core task of CPs. In Figure 8, the distribution of energy quantities for individual classes and charging technologies is plotted. In contrast to the connection duration, differences for the individual classes can be seen in all charging technologies. For example, the median value for AC CEs of class *B. Flatrate* was 27.7 kWh, almost three times higher than for AC CEs of classes *D. Energy* and *E. Mixed* with 10.4 and 10.3 kWh, respectively. In the case of DC and HPC CEs, the results are comparable. Again, class *B. Flatrate* shows the highest amounts of energy transferred with a median of 35.8 kWh for DC and 47.7 kWh for HPC CEs. Interestingly, DC CEs with pricing models of class *C. Time* with a median value of 13.9 kWh had the lowest energy amounts. In the case of HPC CEs, pricing models of classes *A. Free*, *E. Mixed* and *D. Energy* with median values of 10.7, 22.7 and 23.4 kWh, respectively, had the lowest transmitted energy amounts per CE. With pricing models of class *D. Energy*, prices depend directly on the consumed amount of kWh, hence lower amounts of energy transferred can be expected on average. However, this difference is to be regarded as critical from a provider's point of view, because it favors low energy utilization and, in conjunction with long connection durations per CE, inefficient use of the CI. Table A9 shows different percentile values of the transmitted energy amounts per class and charging technology.
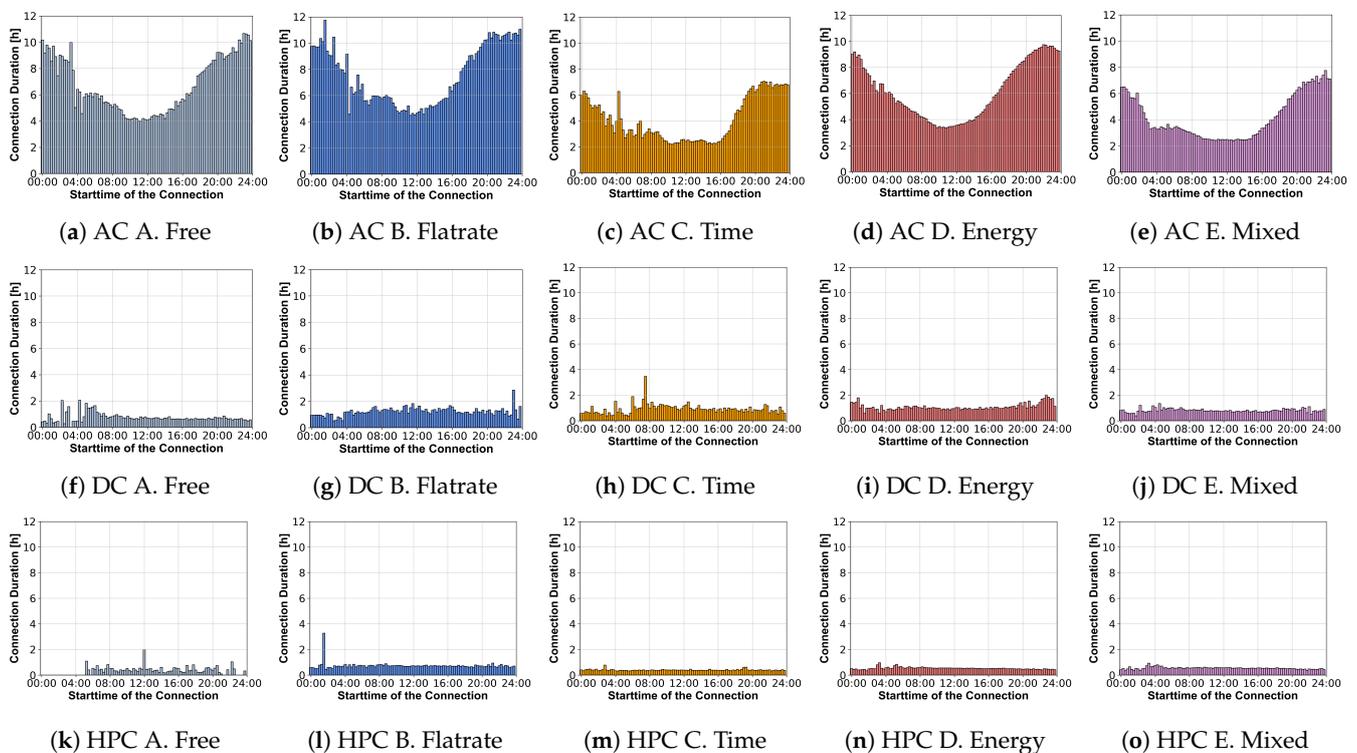

Figure 7. Average connection duration per class of AC, DC, and high-power charging events subject to the start time.

(**a**) AC charging events

(**b**) DC charging events


(**c**) High-power charging events
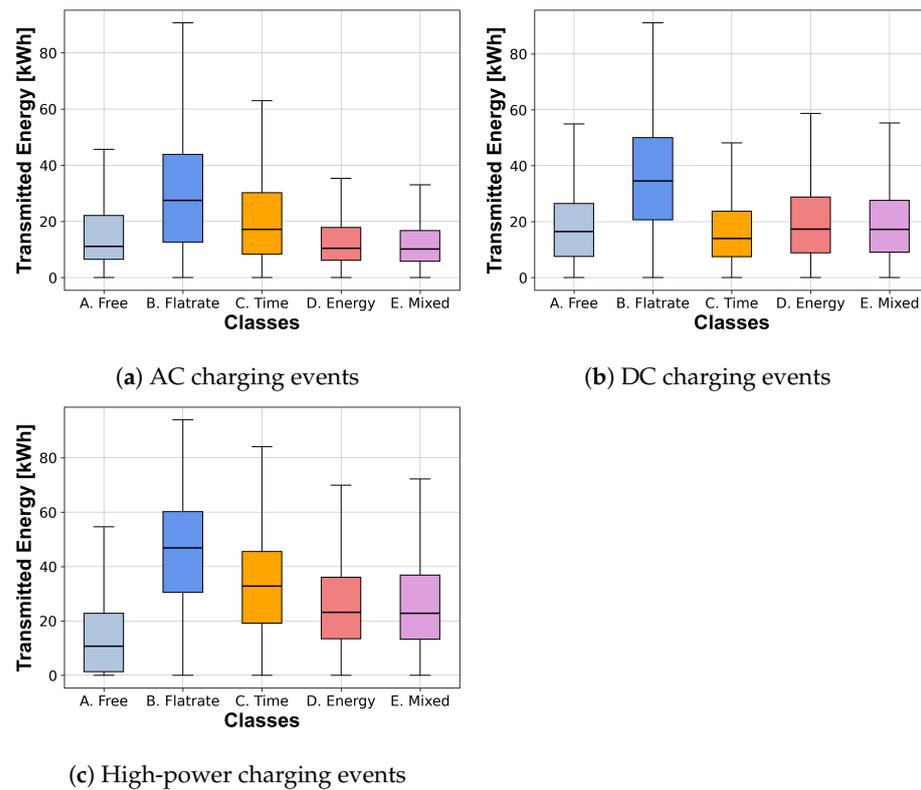
Figure 8. Transmitted energy per pricing model class of AC, DC, and high-power charging events.

For the distributions depicted in Figures 6 and 8 a Kruskal–Wallis one-way analysis of variance was carried out in order to test for each infrastructure type if the distributions of connection duration and transmitted energy per pricing model stemmed from the same distribution [44]. The result of the test showed that the individual distributions of the price models do not originate from the same population. As the Kruskal–Wallis ANOVA only shows the existence of differences, but not between which samples these differences exist, a Mann–Whitney-U test was carried out to test for pairs of distributions of connection duration per pricing model (or transmitted energy, respectively), and if they stemmed from the same population [45]. The results showed that all distributions, with the exception of the energy distribution of HPC CEs of the classes *D. Energy* and *E. Mixed* ($p = 0.53$) are statistically significantly different. The results for the individual distributions are shown in Tables A15–A17 in the Appendix A.

Figures 9 and 10 show the distribution of the connection duration and the amount of energy transferred for individual location types. The median values for the individual price models were determined for this purpose. According to Table A4, the four location types are highway, urban, intermediate, and rural. A maximum distance of 1000 m was selected as the classification feature for the highway location type.

Figure 9 shows the median values of the connection duration. For all location types, CEs with the price model *B. Flatrate* had the longest connection duration. AC CEs of the *B. Flatrate* class at highways and urban charging locations had the longest connection duration, with a median of 5.6 and 5.8 h. In comparison, the connection time for AC CEs with the classes *C. Time* and *E. Mixed* at highways and intermediate charging locations was not even half as long, with a median value of about 2 h. The absolute differences were smaller in the case of DC and HPC CEs. Here, DC CEs of class *B. Flatrate* at intermediate and rural charging locations had a median of 1 h, and HPC CEs with class *C. Time* and *A. Free* on highways had a median of 0.3 and 0.1 h, respectively.

Figure 10 shows the median values of the transferred energy quantities. Here too, CEs of class *B. Flatrate* had the highest values at all location types. HPC CEs of class *B. Flatrate* at urban charging locations had the highest energy quantities, with a median of 52 kWh. In

comparison, HPC CEs of the same class at intermediate charging locations had a median value of 43 kWh, which was around 20% lower. In addition to free DC and HPC CEs of the class *A. Free*, AC CEs of the class *E. Mixed* at highways and intermediate charging locations had the lowest amount of energy, with a median of 10 kWh.
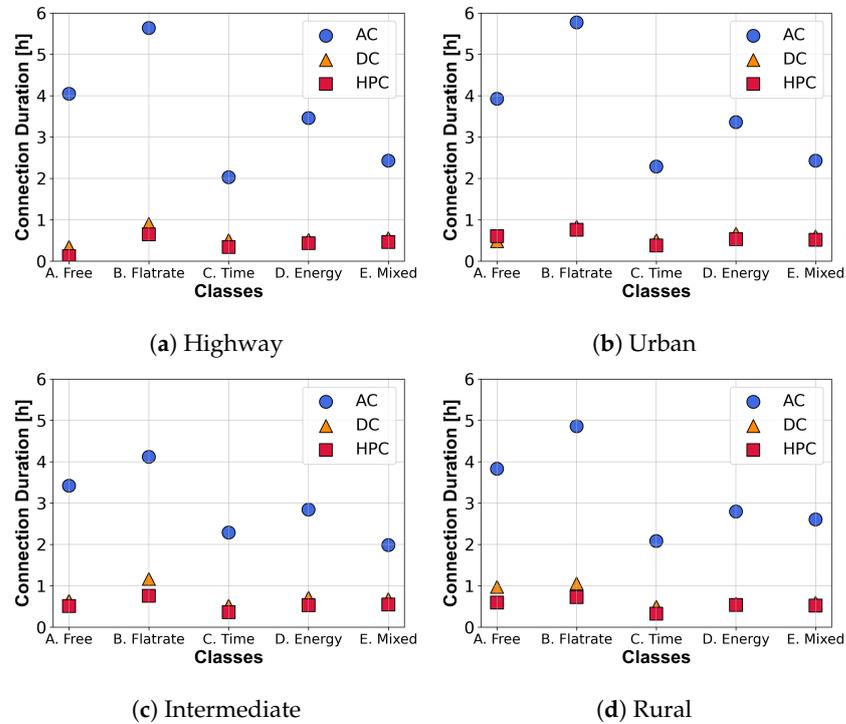

Figure 9. Median connection duration for location types and per pricing model class of AC, DC, and high-power charging events.
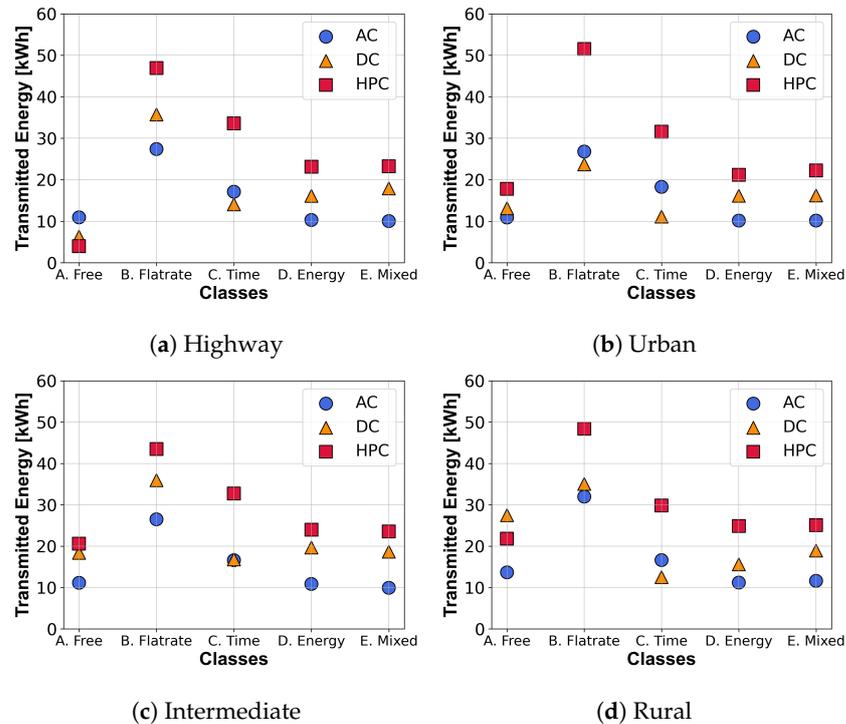

Figure 10. Median transmitted energy for location types and per pricing model class of AC, DC, and high-power charging events.

A more detailed description of the distributions for the individual location types can be found in Figures A7–A10 for the connection duration and in Figures A11–A14 for the energy quantities in Appendix A.

3.2. Charging Behavior

The following section separately investigates the charging behavior for the classified pricing models in more detail. Figure 11 examines the average power of the CEs. It should be noted that the y-axes have been scaled differently by charging technology. The evaluations showed higher values for all charging technologies for the classes *C. Time* and *B. Flatrate* and lower values for classes *D. Energy* and *E. Mixed*. This is interesting, since the average power indicates the proportion of effective charging and idle time. Low average power values can indicate a high proportion of idle time. Therefore, the evaluation results should also be related to the nominal power of CSs as shown in Figure 2 or in Table A6.


(**a**) AC charging events

(**b**) DC charging events

(**c**) High-power charging events
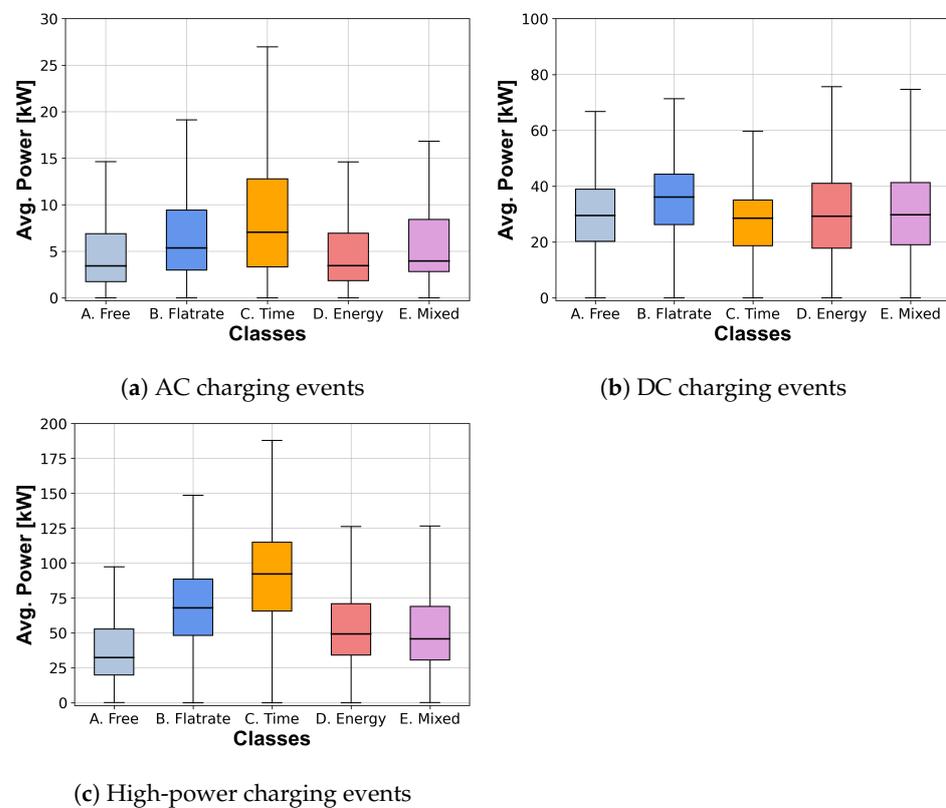
Figure 11. Average charging power per class of AC, DC, and high-power charging events.

In the case of AC CEs, pricing models *C. Time* and *B. Flatrate* featured the highest average charging power, with a median of 7 and 5 kW. In comparison, all other classes had median values between 3 to 4 kW, where about 95% of the AC CPs had a nominal power of 22 kW. In particular, in the case of pricing models with energy-based pricing models of class *D. Energy* and mixed pricing models of *E. Mixed*, this nominal power appeared to be oversized. Thus, the nominal powers of the CPs with 22 kW were more than five times higher than the average powers of these classes with about 4 kW. This is considered important, since over 80% of the AC CEs applied pricing models of classes *D. Energy* and *E. Mixed*.

In the case of DC CEs, the class *B. Flatrate* featured the highest average charging power per CE, with a median of 36 kW. The median values of the other classes were about 30 kW and thus about 15% lower than *B. Flatrate* CEs. The differences between nominal and average power were less pronounced for DC CEs than for AC CEs. For example, the median values were only about 30% to 40% below the prevailing nominal power of 50 kW.

This comparatively low nominal power means that the charging power was often defined by the nominal power of the DC CPs, and the differences between the pricing models were therefore less pronounced.

For HPC CEs, the evaluation shows that with pricing models of the classes *C. Time* and *B. Flatrate*, with median values of 93 and 68 kW, the highest power values could be observed. In comparison, the median values of the other classes, 32 to 50 kW, were 25% to 65% lower than the time-based and flatrate-based pricing models. A large deviation is seen when the average power values are compared to the nominal power values, as with AC CEs. Suppose a nominal power of 300 kW is used as a reference value for the nominal power. In that case, the median values of the average powers are 70% to 90% below the possible nominal power. Thus, the median value of pricing models of class *D. Energy* with ~50 kW is in the range of DC CPs. In comparison, the average charging power of pricing models of class *C. Time* was almost twice as high. Table A10 lists different percentile values per class and charging technology.

In Figure 12, the prices per CE are compared. These prices represent revenues from an EMSP perspective or costs from an e-mobility user's perspective. The prices of CEs of class *A. Free* are always 0 in this evaluation, since charging is cost-free. Due to the nature of class *B. Flatrate*, the CEs in this evaluation tended to show a narrower spread of prices. In addition, in this analysis, the class *E. Mixed* showed the highest prices. The median values here were up to 170% above those of other classes.


(**a**) AC charging events

(**b**) DC charging events

(**c**) High-power charging events
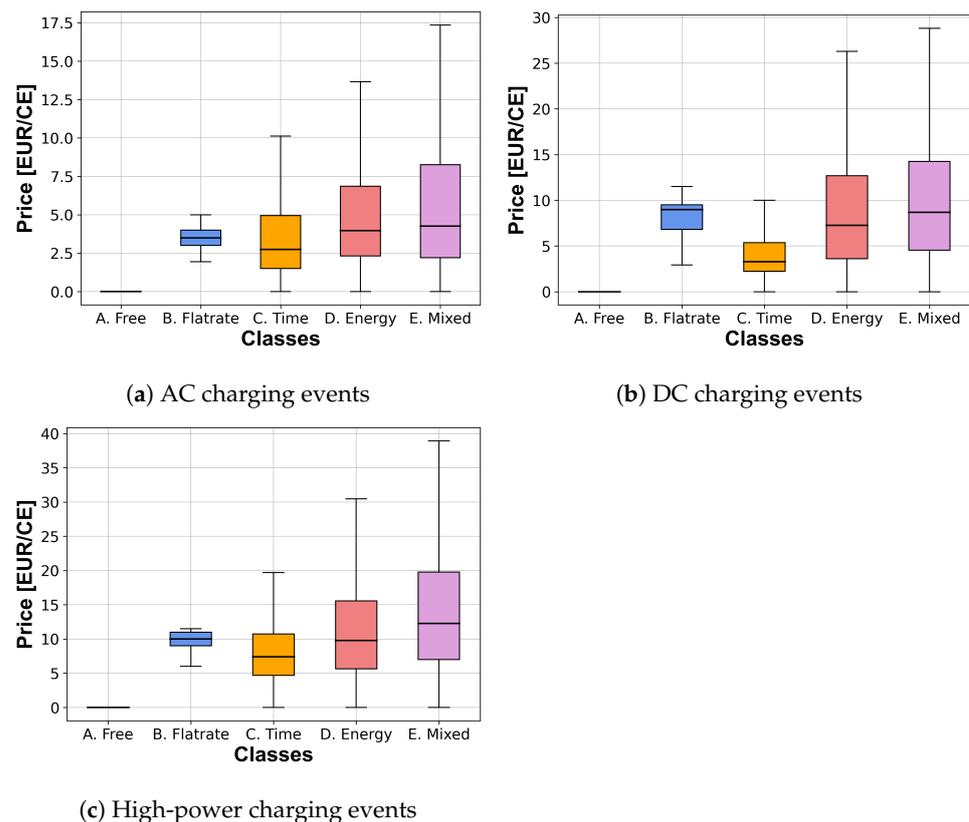
Figure 12. Price per charging event and per class of AC, DC, and high-power charging events.

In order to check if a statistically significant linear relation exists between tariffs and other factors like connection duration, transferred energy, or average power, a correlation analysis was performed. As the information on tariffs is present in the form of dichotomous variables, a point-biserial correlation was employed. Detailed results including *p*-values are presented in Table A14 [46]. All of the correlations were statistically highly significant ($p < 0.01$) but exhibited very low correlations, with strong variation between parameters. For example, the highest correlation, with a value of 0.36, occurred between the average

charging power of HPC CEs and time-based pricing models of class *C. Time*. Hence, from the correlation analyses, only minimal impacts—if any—could be derived. Consequently, further analyses, including additional factors, were required.

As an additional analysis, a density-based spatial clustering of applications with noise (DBSCAN) was performed. This clustering method made it possible to examine the entire dataset with all features used in the study, recognize several clusters, and evaluate the clusters' quality. In addition to the classified five price models, three charging technologies; four location types; and the features connection time, idle time, charging time, amount of energy transferred, price, and average charging power were used. In total, the clustering procedure included 18 features as input parameters. The parameter epsilon for the maximum distance between two samples was chosen so that one was considered to be in the neighborhood of the other, and the min samples for the minimum number of points required to form a dense region were determined iteratively by combining different variants. With an epsilon value of 1.40 and a min sample of 20 points, the clustering procedure resulted in 60 clusters and the silhouette coefficient was maximized with a value of 0.86. The 60 clusters corresponded to the variations of the five classified price models, three charging technologies, and four location types. The high silhouette coefficient showed that classifying price models, charging technologies, and location types made sense. Consequently, the derived clusters represented an analysis of connection time, idle time, charging time, amount of energy transferred, price, and average charging power per combination of price model, charging technology, and location type and correspond to the analyses in Section 3.1.

3.3. Charging or Idling

This section examines the usage patterns of CI in terms of charging and idle times. The charging time describes the period in which the CP transfers energy and the idle time is when the actual charging process has been completed, but the PEV still occupies the CP. The methodology presented in Section 2.3 for estimating the respective temporal proportions was carried through two scenarios. The work at hand employed the average between the two intersection points as an approximation method.

Figure A16 quantifies the charging and idle time separately for AC, DC, and HPC CI. The bar chart in Figure A16a illustrates the relative proportion of charging and idle time, in order to allow comparison with results from other studies. As expected, AC CI shows the highest proportion of idle time at 47%. In other studies, the proportion of idle time was quantified as 45% to 85% [20,21,24,35].

In comparison, the proportion of idle time is much lower for DC and HPC CEs, at 25% and 4%, respectively. In previous studies, the share of idle time in DC and HPC CEs was often not explicitly quantified for these charging technologies, and a mixed value of AC, DC, and HPC charging technologies was given, or the values for idle time were approximate values that did not directly stem from raw data. For example, the share of idle time for DC and HPC CEs was simulatively determined to be ∼10% each [35].

Figure 13 quantifies the share of charging and idle time for the classified price models. As idle time is a relevant parameter for determining the efficiency of public CI, the share of idle time for the individual pricing models is considered and classified below. For the AC CEs in Figure 13a, the price models of the classes *A. Free* and *D. Energy* had the highest share of idle time at around 50% each. In comparison, AC CEs of the classes *C. Time* and *E. Mixed* classes had the lowest share of idle time at 35 and 30%. The share of idle time for DC CEs was lower for all price models. It is interesting to note that CEs of the class *C. Time* had the highest share of idle time of the DC CEs, at 35%. This result is surprising at first glance, as the short connection durations of price models of the class *C. Time* according to Figure 6 for DC CEs indicate efficient use and low idle time. However, it should be noted that this is the relative share and not the absolute value. If the absolute values for the idle time for DC CEs of the class in Table A13 are considered, it can be seen that price models of class *C. Time* had low absolute values compared to the price models of the other classes. The

comparatively high relative share of idle time for DC CEs of class *C. Time* in Figure 13b is thus relativized by the low absolute values of this class. If the shares of unused connection time for HPC CEs are considered in Figure 13c, it can be seen that only HPC CEs of class *A. Free* with 16% had a relevant proportion of idle time. The share of idle time for the price models of the other classes was in the low single-digit range at 2 to 5%. However, also in this case, the relative values must be considered in conjunction with the absolute values of idle time in Table A13. In the case of HPC CEs, all price models of all classes showed comparatively low absolute values for idle time.


(**a**) AC charging events

(**b**) DC charging events

(**c**) High-power charging events
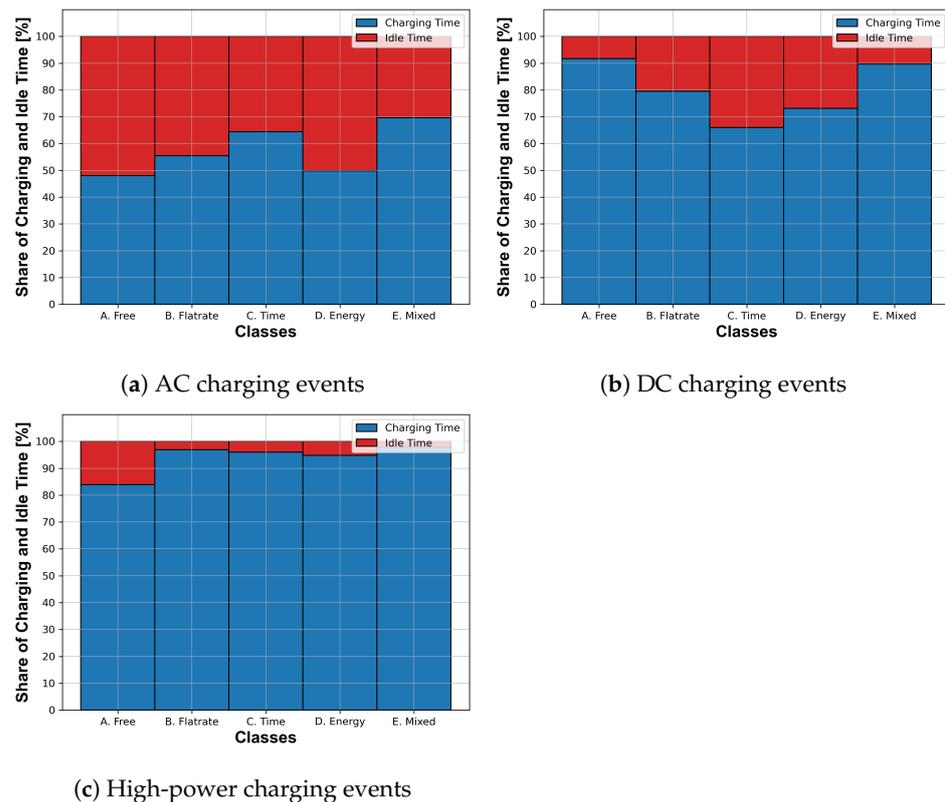
Figure 13. Share of charging and idle time per class of AC, DC, and high-power charging events.

Figure 14 quantifies the charging time in hours for the individual classes. The distribution of charging time is an essential indicator for the design of pricing models. For example, in mixed pricing models, a time-based component can be introduced to separately bill connection durations above typical charging times, thus minimizing idle time. According to the results, such separate pricing is reasonable from 2 h for AC CEs and 0.5 h for DC and HPC CEs. Table A12 quantifies the charging time separately for the individual classes.

Figure 15 shows the connection duration of the CEs as function of the start time of the connection for the individual classes. The values in the diagram reflect the absolute values in Figure 7. However, the connection duration is additionally divided into charging and idle time. For AC CEs, the average charging time is 2.8 h. The length of the charging time is essentially independent of the start time of the connection. Contrary, the length of the idle time differs notably by the start time of the connection. For example, AC CEs of the class *D. Energy* that started between 8 a.m. and 6 p.m. have an average idle time of 2 h, which is only about half the idle time of 4.3 h of CEs that started between 6 p.m. and 8 a.m. Since the connection duration of DC and HPC CEs exhibit less differences with respect to the start time compared to AC CEs, the proportion of charging and idle time is also less characteristic for these charging technologies.

(**a**) AC charging events

(**b**) DC charging events

(**c**) High-power charging events
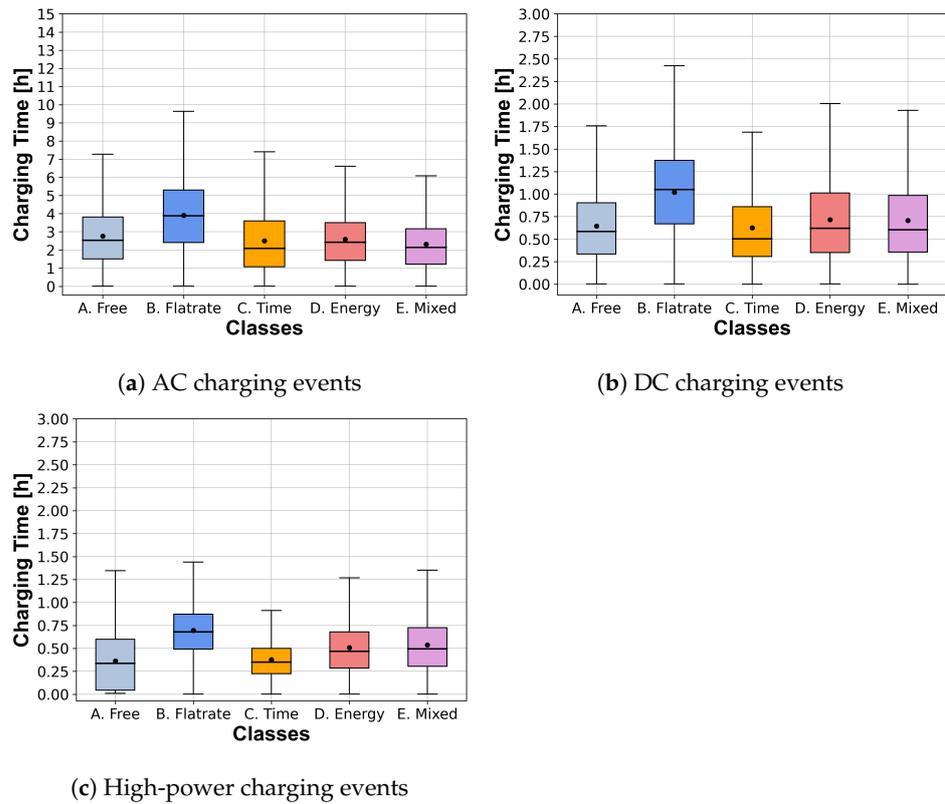
Figure 14. Charging time per class of AC, DC, and high power charging events.

(**a**) AC A. Free　(**b**) AC B. Flatrate　(**c**) AC C. Time　(**d**) AC D. Energy　(**e**) AC E. Mixed

(**f**) DC A. Free　(**g**) DC B. Flatrate　(**h**) DC C. Time　(**i**) DC D. Energy　(**j**) DC E. Mixed

(**k**) HPC A. Free　(**l**) HPC B. Flatrate　(**m**) HPC C. Time　(**n**) HPC D. Energy　(**o**) HPC E. Mixed
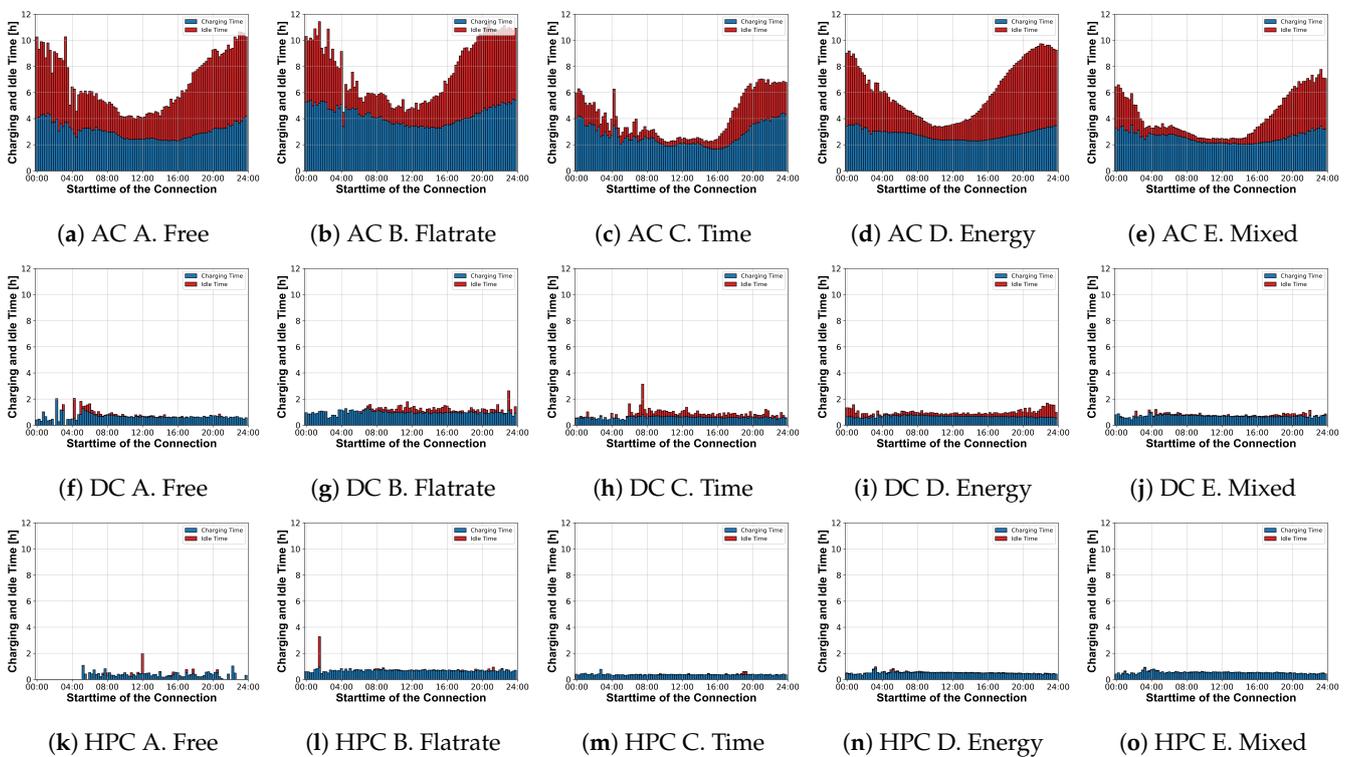
Figure 15. Average charging and idle time per class of AC, DC, and high-power charging events depending on the connection start time.

The study results show the differences in usage behavior when pricing models are considered. The usage behavior was examined based on the performance indicators

connection duration, amount of energy transferred, charging power, revenues, and charging and idle time. The results are ranked in Table 6. The table is an overview of how the values of the classified price models change with different key performance indicators. The class *D. Energy* represented the reference class for the evaluation, since it was the class with the most CEs. The arrows show whether the respective class had a higher, lower, or comparable value compared to energy-based CEs.

Table 6. Direction of effects of pricing models compared to Class D. Energy pricing models.

KPIs	A. Free	B. Flatrate	C. Time	E. Mixed
Connection Duration	↑	↑	↓	↓
Transmitted Energy	↑	↑	↑	→
Avg. Charging Power	↑	↑	↑	→
Revenues	↓	↓	↓	↑
Idle Time	↑	↑	↓	↓

Legend: ↑ Higher, → equal, and ↓ lower values compared to charging events with Class D. energy.

4. Discussion

In the previous sections, differences in charging behavior were investigated with respect to tariff schemes, CI types, and other aspects. This section serves to discuss what these differences mean for different viewpoints on CI usage efficiency. These viewpoints are discussed separately, here. However, when planning the roll-out and utilization of CI, viewpoints on usage efficiency can be combined using a trade-off. In this section, three different viewpoints on efficiency and their goals are described as an example: (1) maximizing the throughput at CIs, (2) optimal interaction between demand for and supply of energy, and (3) revenue maximization. **The first viewpoint on efficiency discussed is increasing the throughput at CI**. This approach pursues the goal of using an existing public CI in a way whereby the largest possible number of PEVs can be supplied with energy. The main goals here are to minimize the connection time per CE and to simultaneously increase the energy quantity transferred. Due to their higher charging power, DC and HPC CIs have much shorter connection durations and can simultaneously transmit higher energy quantities than AC CIs. Considering the 50% percentile value for pricing models of class *D. Energy* (see Table A8), it can be seen that AC CEs with 3.25 h have a connection duration that is longer by a factor of 5 to 7 than DC and HPC CEs with 0.64 and 0.47 h, respectively. Therefore, in order to reduce the connection time per connection and, at the same time, increase the number of possible connections per CI, the construction of DC and HPC CIs seems to be reasonable. An interesting aspect becomes apparent when the pricing models within DC or HPC CI are considered. By using pricing models of the class *C. Time*, the connection duration can be reduced to 0.50 and 0.36 h, respectively, which represents a further reduction of about 30%. At the same time, the evaluation in Table A9 shows that high energy quantities of about 34 kWh per CE can be transmitted when certain pricing models are implemented for HPC CEs. Consequently, building CIs with high charging power and using pricing models of class *C. Time* can be considered a promising approach to increase throughput at public CI.

The second viewpoint on efficiency considered is the avoidance of peaks in power demand. The main objective here is to mitigate demand, in order to avoid network breakdowns and reduce the need for grid extensions. This mitigation can be achieved by two approaches: shifting CEs to low-demand periods or stretching the active charging time over a longer period of time. One approach to measuring temporal flexibility is to observe the presence of idle time. A comparison of charging technologies shows that AC CEs have a high share of idle time. When the 50% percentile value for energy-based pricing models is considered (see Table A10), it can be seen that AC CEs have an average power of about 3 kW. In comparison, the average power of DC and HPC CEs is about 30 and 50 kW, respectively, which is a factor of 10 to 17. At the same time, the 50% percentile value in Table A13 shows that energy-based AC CEs have about 0.8 h of idle time per CE. Comparing the

pricing models, the classes *B. Flatrate* and *A. Free* with about 1 h of idle time per CE show a higher value by about 20%. Figure 15 shows that idle time is especially high between 6 p.m. and 8 a.m., providing significant potential to mitigate peak power during these periods by stretching CEs. In a slightly different approach, the idle time could also be used for so-called "vehicle-to-grid" approaches [47]. In summary, building AC CI appears promising for reducing peak power demand. In particular, pricing models of the classes *B. Flatrate* and *A. Free* offer the possibility of using the vehicle batteries for additional system services and thus to develop further revenue streams. In terms of shifting power demand over time, DC and HPC CI show less potential. However, it is conceivable that DC and HPC CEs, in conjunction with coupled storage systems, could create flexibility here.

The third viewpoint on efficiency is revenue maximization. The objective here is to increase the revenues for CPOs or EMSPs and thus ensure the amortization of public CI and, for example, enable the roll-out of public CI without subsidies. In addition to the revenue per CE, the number of feasible CEs per CI is also important. With regard to the revenues per CE, it is evident that higher revenues can be realized through DC or HPC CI. Considering the 50% percentile value in Table A11, it becomes evident that for DC and HPC CEs with about 7 and 10 Euro per CE, respectively, about twice as much revenue per CE can be realized as in AC CEs with about 4 Euro per CE. If the price models are compared, it can be seen that the revenues can be additionally increased by price models of class *E. Mixed*. In comparison, time-based pricing models of class *C. Time* show consistently lower revenues. An interesting point here is that it is conceivable that time-based pricing models can generate higher total revenues despite lower revenues per CE, since time-based pricing models enable a higher throughput of CEs. However, since the dataset used in this study does not include all CEs per CI, no conclusive assessment can be made regarding the profitability of different approaches for public CI. The economics of different approaches to CI and pricing models can thus be the subject of future research, which may be based on simulations or real-world experiments. Future studies should also consider the higher capital and operating costs for DC and HPC CI [28,35].

5. Conclusions

This study was the first to investigate how public CI usage differs under the presence of diverse pricing models. For this purpose, a comprehensive EMSP dataset of approx. 3 million CEs from 2020 to 2022 from various European countries was used. Compared to previous studies, the EMSP dataset includes information on the charging tariff in addition to general information about the CEs. Depending on the price composition, the CEs were classified into the five price models *A. Free*, *B. Flatrate*, *C. Time*, *D. Energy*, and *E. Mixed* and evaluated based on the performance indicators connection duration, transferred energy volume, average charging power, achievable revenue, and the charging and idle time proportion for AC DC and HPC CI. The study results indicated that the performance indicators differed for the classified pricing models. In addition to the quantitative comparison of the performance indicators, a Kruskal–Wallis one-way analysis and a pairwise comparison using the Mann–Whitney-U test proved that the data distributions of the price models determined were statistically significantly different.

However, it should be noted that no causal relationship between the pricing models and user behavior can be drawn from the present studies, as this is not possible due to the nature of the dataset. As in previous studies, it can be determined based on the available billing data and statistical methods that usage behavior differed significantly for individual data distributions. However, it is impossible to derive a direct causal relationship on this basis alone, as information about the user or the selection procedure for the pricing system is missing. However, as the authors do not have the motives behind the users' choice of tariff, no causality can be inferred here.

At this point, further limitations of the present study are discussed. Since the dataset used is only an excerpt from the overall use of the individual CSs, this study does not aim to make statements about the economic efficiency, overall load profile, or usage behavior of

individual CSs. Another limitation in the data analysis was the high proportion of CEs from Germany (70%) and the high proportion of energy-based pricing models of class *E. Energy* (66%). In this context, the available EMSP dataset was compared with the CPO dataset of Stadtwerke München (SWM), the city's largest provider of public CI, using Munich as an example. The comparison of the data distributions in Figure A1 in the Appendix A shows that the EMSP dataset and the CPO dataset had similar data distributions. It should be noted here that 99% of the intersection of the CEs were price models of class *D. Energy*. Since only the necessary data for the city of Munich, and thus for a selected application area, were available for such a comparison, future work is required based on similar datasets, to ensure the transferability of the results to other application areas and price models other than class *D. Energy*.

Nonetheless, some implications for the different pricing models can be derived when comparing to pricing model *D. Energy* as reference: pricing models *A. Free* and *B. Flatrate* exhibited CEs with higher connection durations due to longer idle times. While it is not favored by CP operators, such behavior with both pricing models could be a lever to foster "Vehicle-to-Grid" approaches, as well as mitigating peak power, especially overnight. With pricing model *C. Time*, lower idle times were present and therefore shorter connection durations with its CEs, as well as higher avgerage charging power with lower revenues per CE. This behavior allows more vehicles to be charged per CP, due to the availability gained, offsetting the reduction in revenues per CE, but detering charging overnight. Finally, *E. Mixed* pricing models, as seen in the dataset, seem to blend the benefits of time-based and energy-based pricing models. While idle times, and therefore connection durations, are lower compared to energy-based models, revenues are higher due to the fact that low-energy charging behavior is priced via a time-based component. With this pricing model, just like with time-based models, vehicle throughput is larger. Further on, this type of pricing model could enable the operator to better monetize the different charging behaviors and therefore to increase revenue per CE. This study shows differences in charging behavior for different pricing models, which could be relevant parameters for public CI. The results of this study enable a more in-depth understanding of pricing mechanisms in connection with public CI.

Based on the existing study results and limitations, three possible starting points for future studies are described below. (1) In future studies, datasets could be combined with qualitative surveys of users to gain further insights. In this way, a link could be established between users' preferences for charging PEVs and datasets that do not contain detailed information about the user or the reasons for their decision. Based on such studies, it could be determined under which specific framework conditions certain pricing models are preferred or whether the selection of pricing models depends on individual charging technologies or charging locations. Future developments, such as technological progress and the interaction between private and public charging infrastructure, should also be considered. For example, it remains to be seen how increasing battery capacities and higher charging power of PEVs could affect public CI demand and usage behavior [48]. Furthermore, the change in the availability of CI at private or semi-public locations such as park and ride facilities or CPs at workplaces could have an impact on usage behavior at public CI. (2) Due to the dataset used, the effects of the various pricing models on the energy grid could not be investigated. Future studies could pick up here and investigate the relationships between pricing models, the required public CI in possible scaling strategies, and the repercussions for the energy grid. The price models investigated consider comparatively simple variables such as the connection duration or the amount of energy transferred. By considering additional variables such as the current utilization of the local energy grid or the share of renewable energy, pricing models could be used to optimize the utilization of the energy grid through monetary incentives [49,50]. (3) Another aspect of future research lies in testing different pricing models. Here, experimental trials on a limited temporal and spatial scale and accompanying research in model areas could provide information on the population's acceptance of the pricing models and the control effect.

Appendix A

(**a**) Connection duration of AC charging events

(**b**) Connection duration of DC charging events
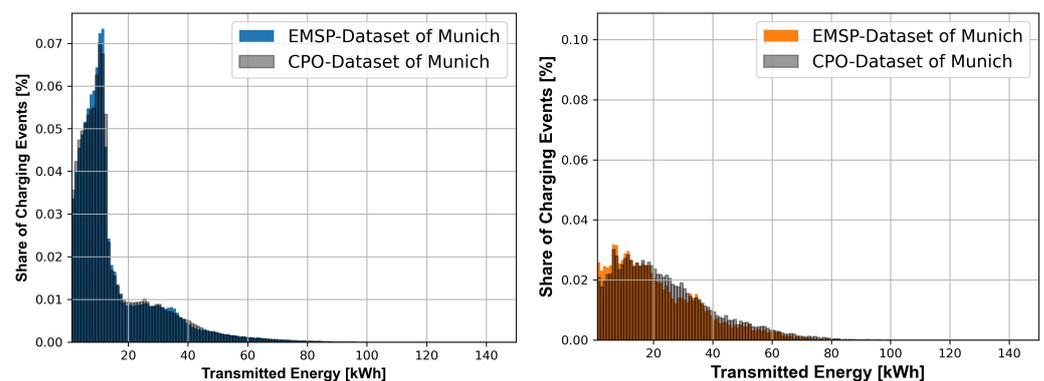
(**c**) Transmitted energy of AC charging events

(**d**) Transmitted energy of DC charging events

Figure A1. Comparison EMSP- and CPO-dataset of Munich regarding connection duration and transmitted energy of AC and DC charging events.

(**a**) Charging events 2020

(**b**) Charging events 2021

(**c**) Charging events 2022
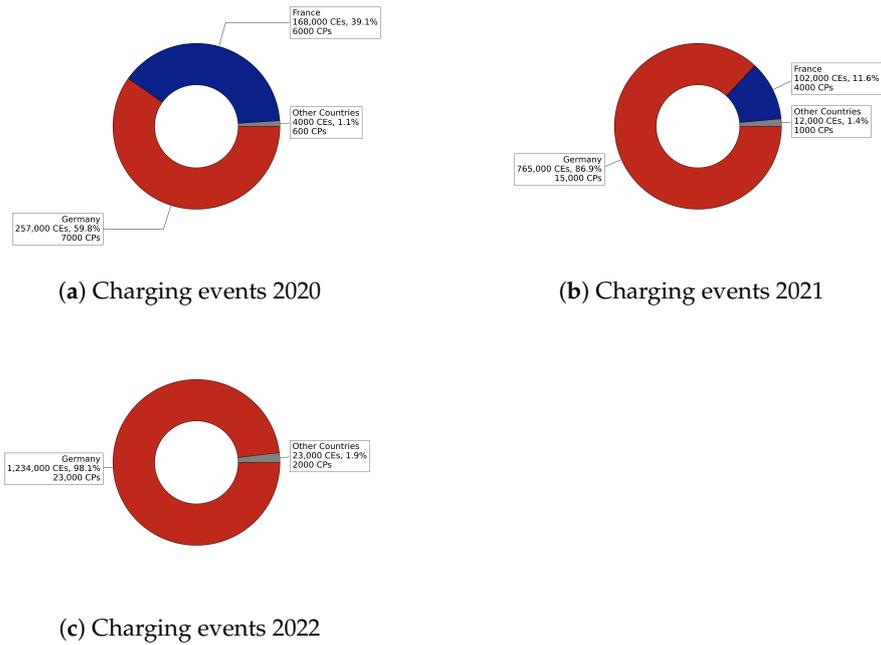
Figure A2. Number of charging events per country and period of time in the dataset.

Table A1. KPIs of AC charging events from the real-world dataset per country.

Country	Number of CPs	Number of CEs	Power Range [kW]	Avg./Median Con. Duration [h/CE]	Avg./Median Energy [kWh/CE]
Germany	20,000	2 m	3–43	4.9/3.1	14.8/10.5
France	5900	240,600	3–43	4.2/2.2	18.8/15.2

Table A2. KPIs of DC charging events from the real-world dataset per country.

Country	Number of CPs	Number of CEs	Power Range [kW]	Avg./Median Con. Duration [h/CE]	Avg./Median Energy [kWh/CE]
Germany	2600	89,000	22–140	0.9/0.6	22.5/19.1
France	600	20,700	22–50	0.8/0.5	16.1/12.4

Table A3. KPIs of high-power charging events from the real-world dataset per country.

Country	Number of CPs	Number of CEs	Power Range [kW]	Avg./Median Con. Duration [h/CE]	Avg./Median Energy [kWh/CE]
Germany	4200	100,000	150–360	0.5/0.5	28.3/25.2
France	200	500	175–350	0.5/0.5	34.8/34.7

Table A4. Share of charging locations according to the classes highway, predominantly urban, intermediate, and predominantly rural.

Charging Technology	Distance to Highway [m]	Highway [%]	Urban [%]	Intermediate [%]	Rural [%]
AC	500	5.1	43.4	35.3	16.2
DC	500	27.7	22.4	28.2	21.7
HPC	500	41.9	22.6	26.8	8.7
AC	1000	9.9	40.4	34.0	15.7
DC	1000	36.6	19.0	24.2	20.3
HPC	1000	53.6	18.5	21.4	6.6

Table A4. *Cont.*

| Charging Technology	Distance to Highway [m]	Highway [%]	Urban [%]	Intermediate [%]	Rural [%]
AC	2000	21.5	32.9	30.7	14.9
DC	2000	45.9	14.5	21.6	18.0
HPC	2000	61.7	14.5	18.0	5.8

Table A5. Parameter for modeling of the charging areas.

Charging Technology	Charging Area	Max. Battery Capacity	Min. Battery Capacity
AC	3 kW (16 A 1 Phase)	20 kWh	5 kWh
AC	4 kW (20 A 1 Phase)	40 kWh	20 kWh
AC	7 kW (16 A 2 Phases)	80 kWh	40 kWh
AC	11 kW (16 A 3 Phases)	150 kWh	40 kWh
AC	16 kW (24 A 3 Phases)	150 kWh	40 kWh
AC	22 kW (32 A 3 Phases)	150 kWh	40 kWh
DC	50 kW	150 kWh	40 kWh
DC	80 kW	150 kWh	40 kWh
DC	100 kW	150 kWh	40 kWh
DC	120 kW	150 kWh	40 kWh
DC	140 kW	150 kWh	40 kWh
HPC	150 kW	100 kWh	60 kWh
HPC	180 kW	100 kWh	60 kWh
HPC	200 kW	120 kWh	70 kWh
HPC	250 kW	120 kWh	80 kWh
HPC	270 kW	120 kWh	80 kWh
HPC	300 kW	150 kWh	80 kWh
HPC	350 kW	150 kWh	80 kWh
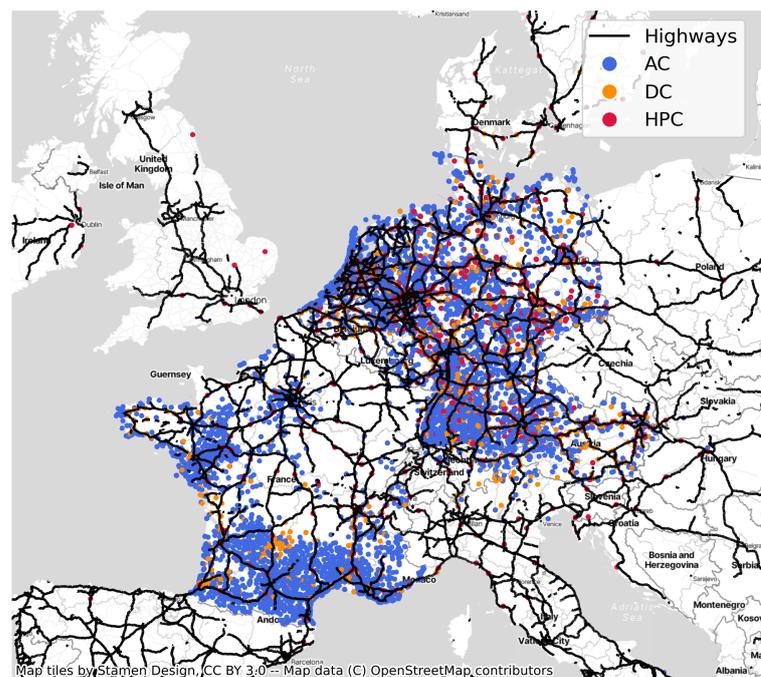
(**a**) Highways

Figure A3. *Cont.*
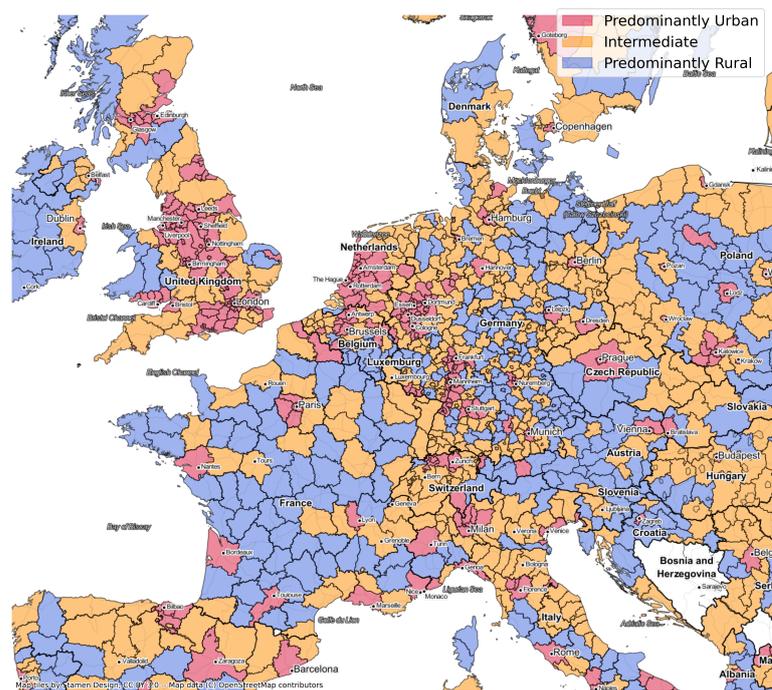
(**b**) Urban and Rural typology

Figure A3. European highways and urban and rural typology.
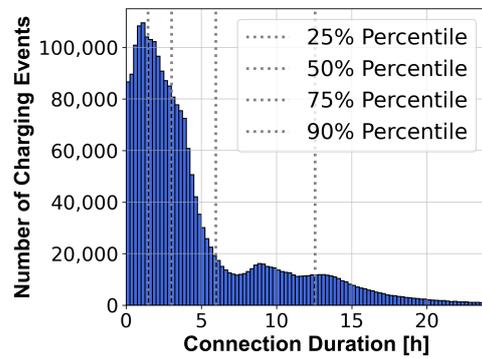
(**a**) AC charging events
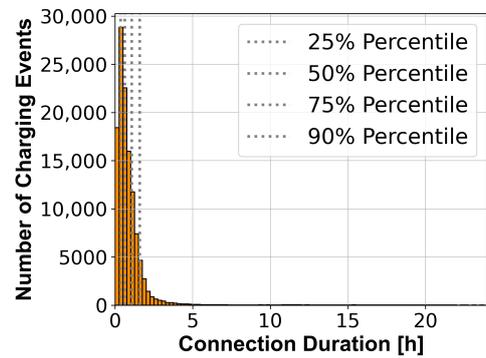
(**b**) DC charging events
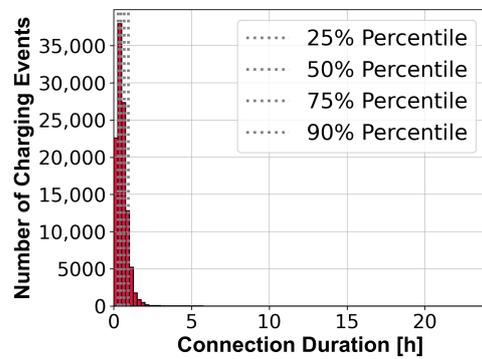
(**c**) High-power charging events

Figure A4. Connection duration of AC, DC, and high-power charging events.

(**a**) AC Charging Events

(**b**) DC charging events

(**c**) High-power charging events
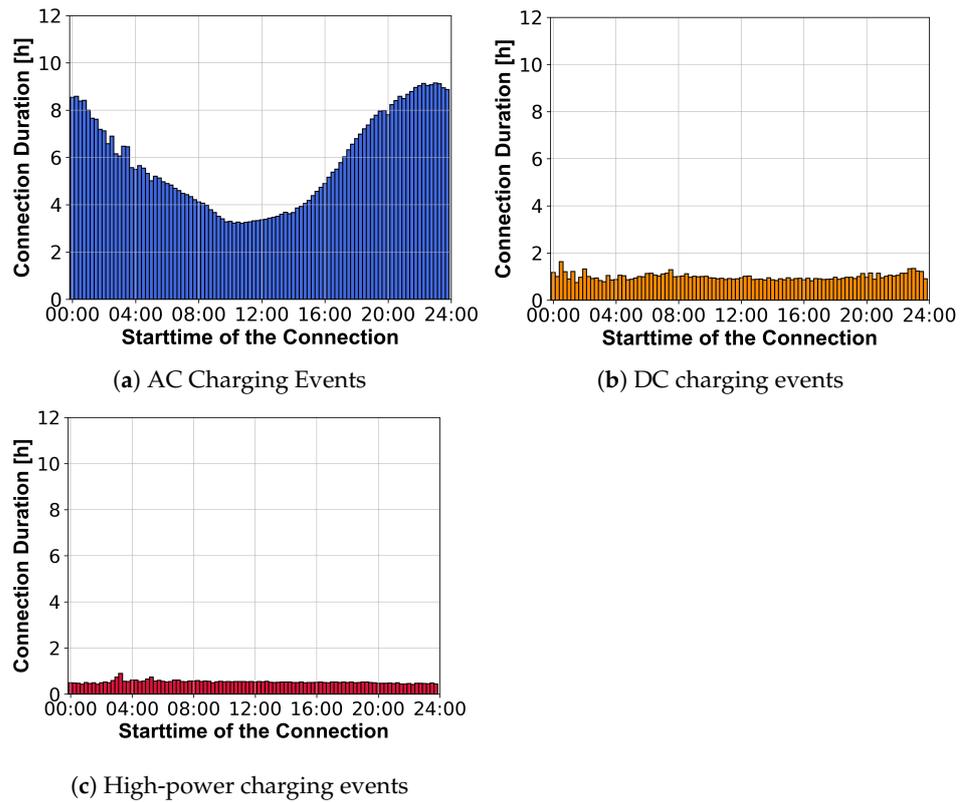
Figure A5. Average connection duration of AC, DC, and high-power charging events depending on the connection start time.

(**a**) AC charging events

(**b**) DC charging events

(**c**) High-power charging events
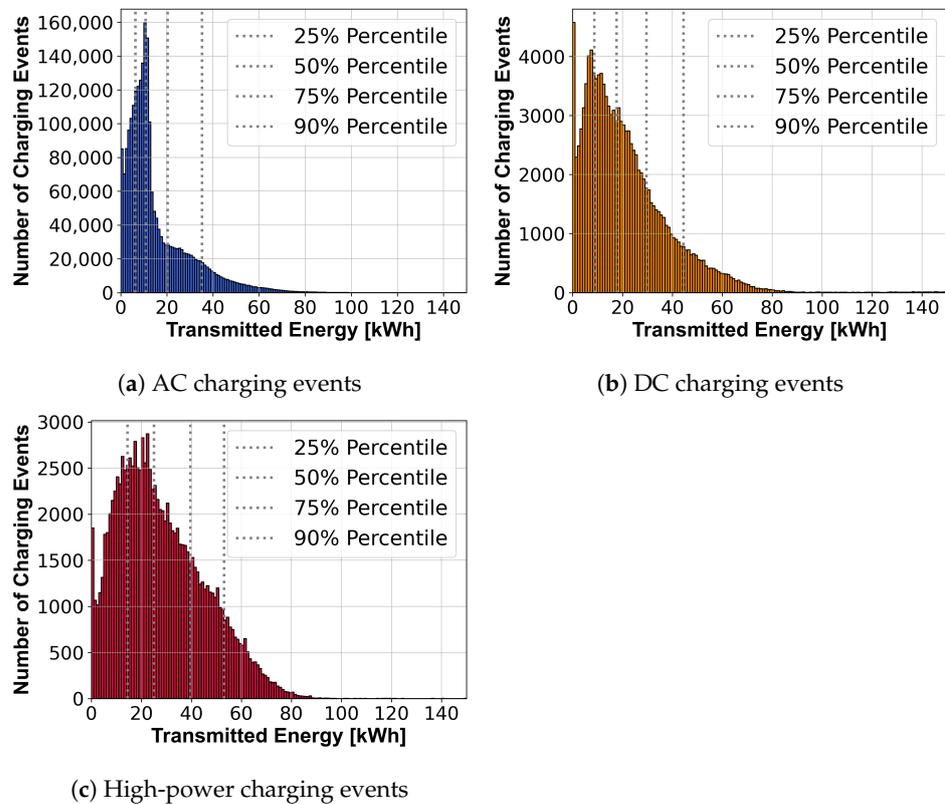
Figure A6. Transmitted energy of AC, DC and high-power charging events.
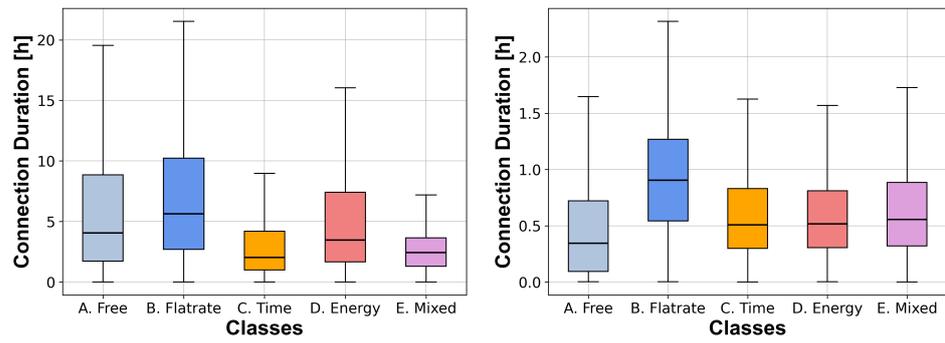
(**a**) AC charging events

(**b**) DC charging events
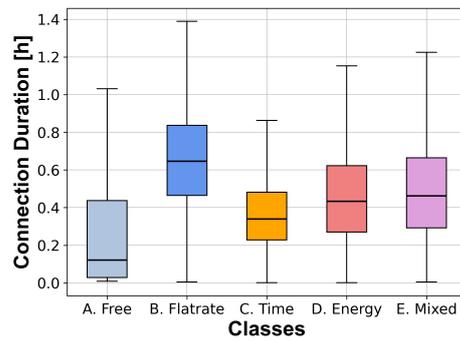
(**c**) High-power charging events

Figure A7. Connection duration for location type highway per pricing model class of AC, DC, and high-power charging events.
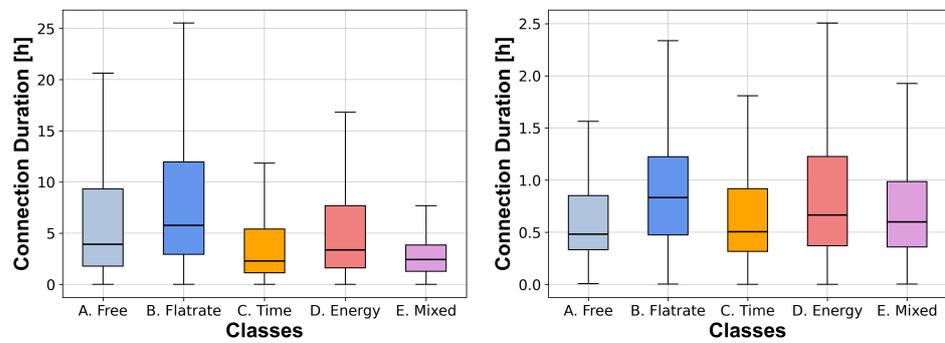
(**a**) AC charging events

(**b**) DC charging events
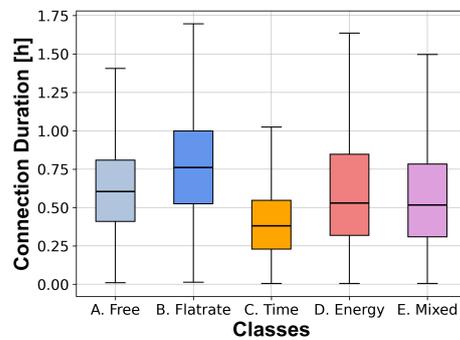
(**c**) High-power charging events

Figure A8. Connection duration for location type urban per pricing model class of AC, DC, and high-power charging events.
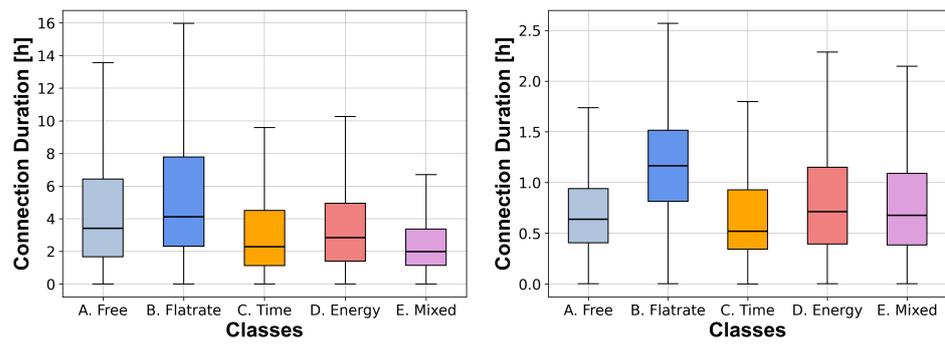
(**a**) AC charging events

(**b**) DC charging events
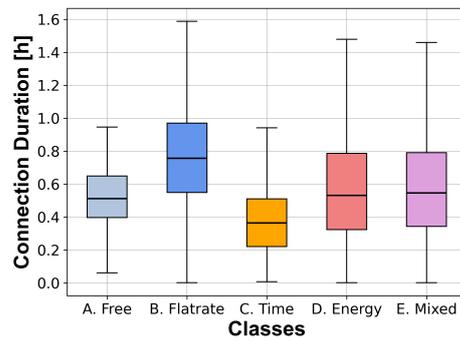
(**c**) High-power charging events

Figure A9. Connection duration for location type intermediate per pricing model class of AC, DC, and high-power charging events.
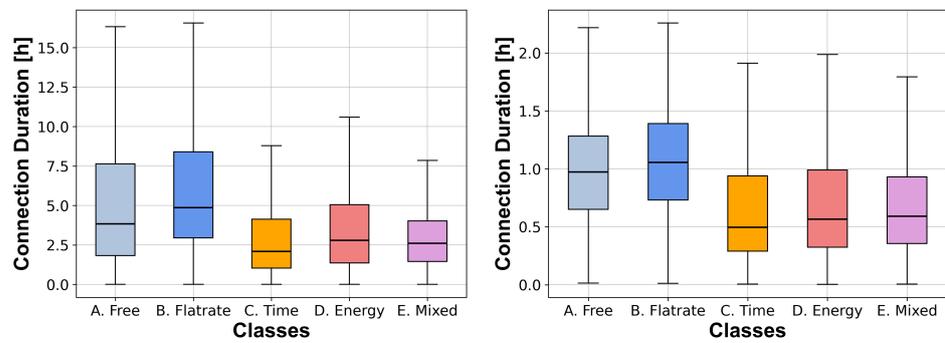
(**a**) AC charging events

(**b**) DC charging events
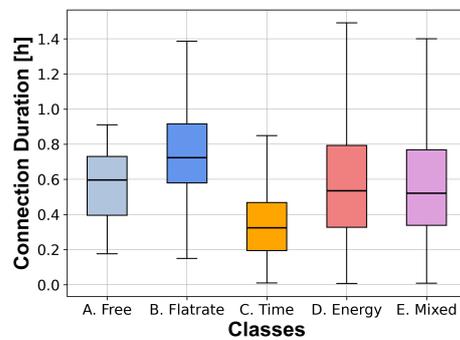
(**c**) High-power charging events

Figure A10. Connection duration for location type rural per pricing model class of AC, DC, and high power charging events.
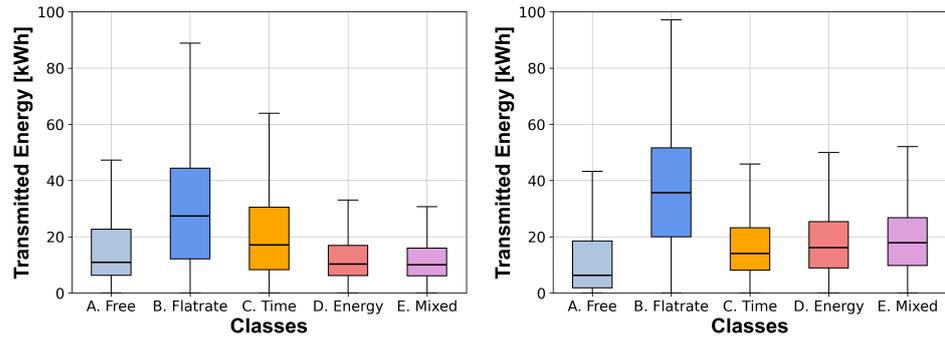
(**a**) AC charging events

(**b**) DC charging events
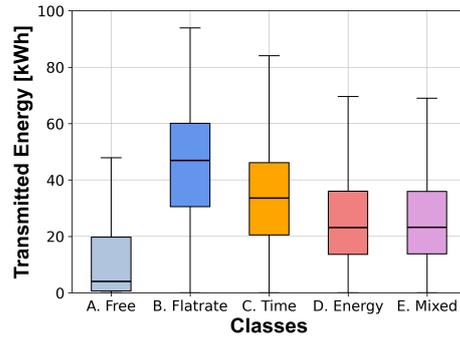
(**c**) High-power charging events

Figure A11. Transmitted energy for location type highway per pricing model class of AC, DC, and high-power charging events.
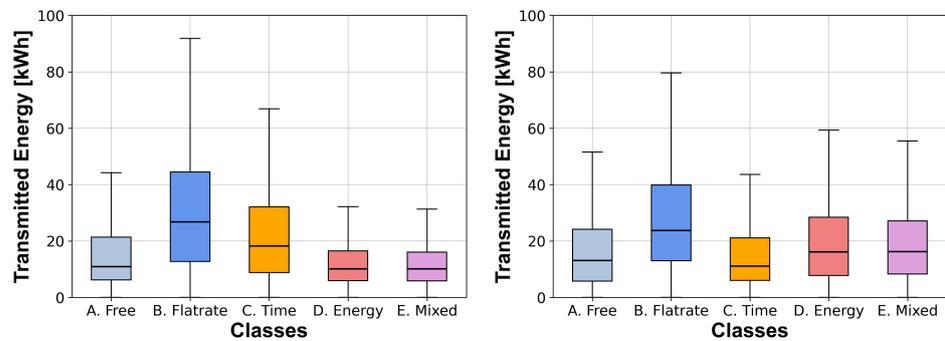
(**a**) AC charging events

(**b**) DC charging events
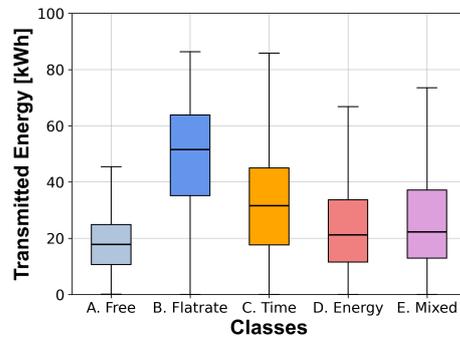
(**c**) High-power charging events

Figure A12. Transmitted energy for location type urban per pricing model class of AC, DC, and high-power charging events.
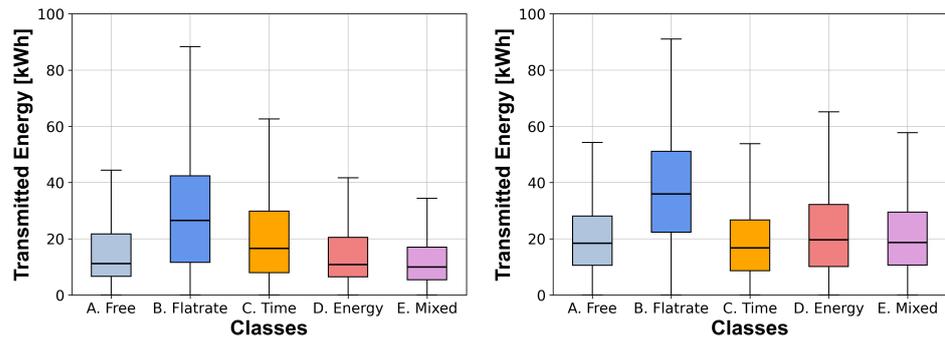
(**a**) AC charging events

(**b**) DC charging events
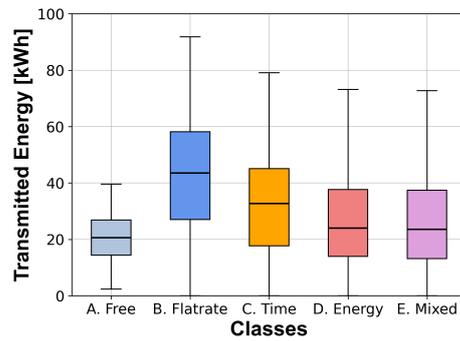
(**c**) High-power charging events

Figure A13. Transmitted energy for location type intermediate per pricing model class of AC, DC, and high-power charging events.
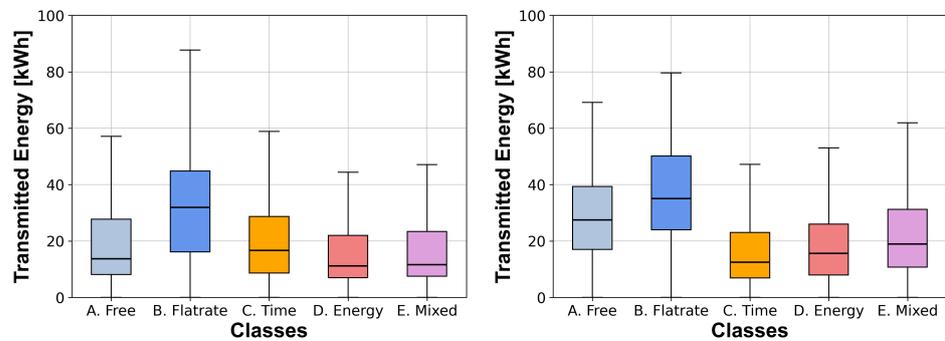

(**a**) AC charging events

(**b**) DC charging events
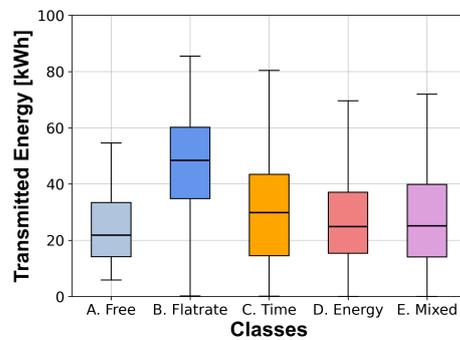
(**c**) High-power charging events

Figure A14. Transmitted energy for location type rural per pricing model class of AC, DC, and high-power charging events.

Table A6. Nominal charging power for AC, DC and high-power charging events from the real-world dataset.

Charging Technology	Percentil 25% [kW]	Percentil 50% [kW]	Percentil 75% [kW]	Percentil 90% [kW]	Percentil 95% [kW]
AC	22	22	22	22	22
DC	50	50	50	53	75
HPC	150	300	300	350	350

Table A7. Average charging power for AC, DC, and high-power charging events from the real-world dataset.

Charging Technology	Percentil 25% [kW]	Percentil 50% [kW]	Percentil 75% [kW]	Percentil 90% [kW]	Percentil 95% [kW]
AC	2.1	3.6	7.3	11.0	15.0
DC	19.8	31.2	42.2	48.2	61.3
HPC	36.0	54.6	81.1	110.3	126.0
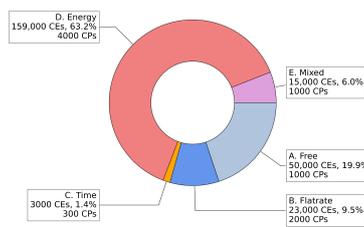
(**a**) Classes Germany 2020
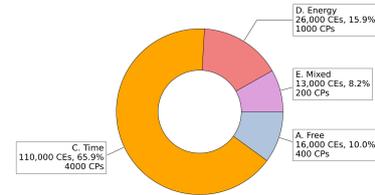
(**b**) Classes France 2020
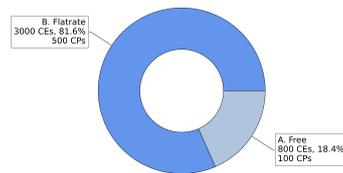
(**c**) Classes other countries 2020
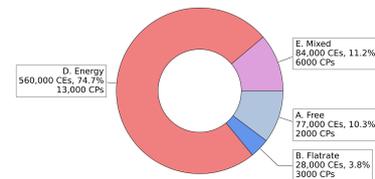
(**d**) Classes Germany 2021
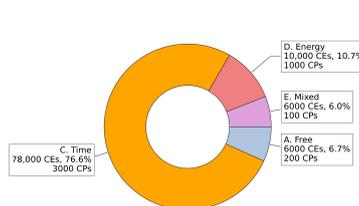
(**e**) Classes France 2021
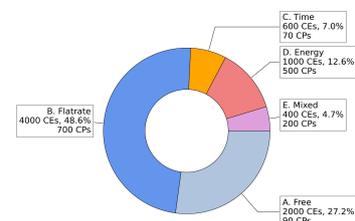
(**f**) Classes other countries 2021

Figure A15. *Cont.*

(**g**) Classes Germany 2022   (**h**) Classes Other Countries 2022
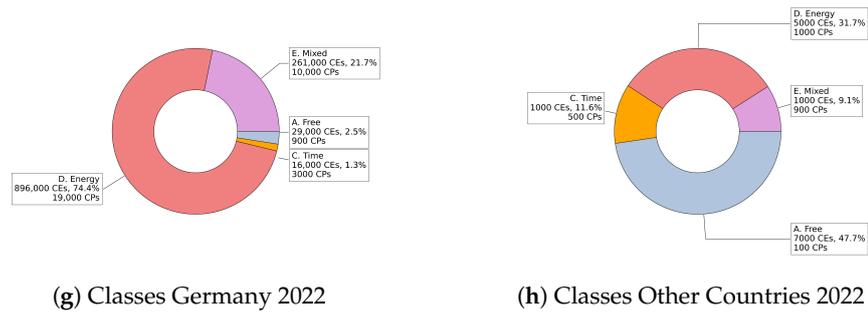
Figure A15. Distribution of the classified pricing models per country and period of time in the dataset.

Table A8. Connection duration per pricing model class for AC, DC, and high-power charging events.

Charging Technology	Class	Percentil 25% [h]	Percentil 50% [h]	Percentil 75% [h]	Percentil 90% [h]	Percentil 95% [h]
AC	A. Free	1.70	3.63	8.09	13.55	17.13
AC	B. Flatrate	2.70	4.90	9.92	14.80	17.93
AC	C. Time	1.10	2.20	4.47	10.52	12.48
AC	D. Energy	1.58	3.25	6.77	13.26	16.12
AC	E. Mixed	1.26	2.35	3.75	7.55	11.72
DC	A. Free	0.33	0.58	0.91	1.25	1.51
DC	B. Flatrate	0.71	1.09	1.45	1.82	2.50
DC	C. Time	0.30	0.50	0.89	1.44	1.98
DC	D. Energy	0.36	0.64	1.08	1.68	2.37
DC	E. Mixed	0.36	0.60	1.01	1.48	1.82
HPC	A. Free	0.04	0.34	0.60	0.83	1.03
HPC	B. Flatrate	0.50	0.69	0.88	1.09	1.27
HPC	C. Time	0.25	0.36	0.51	0.65	0.76
HPC	D. Energy	0.29	0.47	0.69	0.96	1.16
HPC	E. Mixed	0.31	0.49	0.73	0.98	1.15

Table A9. Transmitted energy per class for AC, DC, and high-power charging events.

Charging Technology	Class	Percentil 25% [kWh]	Percentil 50% [kWh]	Percentil 75% [kWh]	Percentil 90% [kWh]	Percentil 95% [kWh]
AC	A. Free	6.38	11.04	21.96	36.83	46.67
AC	B. Flatrate	12.75	27.70	44.31	59.54	66.72
AC	C. Time	8.59	17.37	30.35	41.93	49.62
AC	D. Energy	6.24	10.42	17.95	33.41	42.20
AC	E. Mixed	5.9	10.26	16.84	31.36	39.88
DC	A. Free	7.56	16.39	26.42	39.66	48.96
DC	B. Flatrate	22.07	35.78	51.11	62.96	68.77
DC	C. Time	7.45	13.86	23.97	36.36	45.50
DC	D. Energy	9.26	17.69	29.02	42.64	51.49
DC	E. Mixed	9.38	17.60	28.05	39.76	47.95
HPC	A. Free	1.16	10.71	22.65	37.90	49.12
HPC	B. Flatrate	31.82	47.74	60.72	69.40	73.88
HPC	C. Time	21.40	34.26	46.50	55.55	60.34
HPC	D. Energy	13.77	23.38	36.21	49.26	56.92
HPC	E. Mixed	13.27	22.68	30.54	50.43	57.67

Table A10. Average charging power per class for AC, DC, and high-power charging events.

Charging Technology	Class	Percentil 25% [kW]	Percentil 50% [kW]	Percentil 75% [kW]	Percentil 90% [kW]	Percentil 95% [kW]
AC	A. Free	1.74	3.42	6.90	10.59	12.55
AC	B. Flatrate	3.00	5.39	9.48	11.19	15.14
AC	C. Time	3.35	7.09	12.89	17.65	19.98
AC	D. Energy	1.86	3.46	6.96	10.72	11.96
AC	E. Mixed	2.81	3.92	8.33	11.13	15.74
DC	A. Free	20.22	29.53	38.94	45.91	47.65
DC	B. Flatrate	26.59	36.33	44.37	46.83	48.97
DC	C. Time	19.25	28.53	34.90	40.52	43.50
DC	D. Energy	18.13	29.63	41.21	46.27	48.65
DC	E. Mixed	19.00	29.76	41.30	46.23	48.53
HPC	A. Free	19.90	32.34	52.78	79.60	87.89
HPC	B. Flatrate	48.83	68.23	88.62	112.88	125.79
HPC	C. Time	66.95	93.10	115.02	133.12	142.67
HPC	D. Energy	34.47	49.60	71.20	98.54	116.74
HPC	E. Mixed	30.58	45.70	69.02	94.57	110.13

Table A11. Price per CE and per class for AC, DC, and HPC CEs.

Charging Technology	Class	Percentil 25% [Euro/CE]	Percentil 50% [Euro/CE]	Percentil 75% [Euro/CE]	Percentil 90% [Euro/CE]	Percentil 95% [Euro/CE]
AC	A. Free	0	0	0	0	0
AC	B. Flatrate	3.00	3.50	4.38	6.00	6.82
AC	C. Time	1.50	2.73	4.95	8.43	11.94
AC	D. Energy	2.34	3.98	6.88	12.97	16.91
AC	E. Mixed	2.24	4.28	8.31	15.34	20.80
DC	A. Free	0	0	0	0	0
DC	B. Flatrate	7.00	9.00	9.50	11.00	11.50
DC	C. Time	2.27	3.27	5.21	8.30	11.31
DC	D. Energy	3.76	7.37	12.74	19.70	24.53
DC	E. Mixed	4.54	8.68	14.26	21.02	26.01
HPC	A. Free	0	0	0	0	0
HPC	B. Flatrate	9.00	9.99	11.00	15.00	15.00
HPC	C. Time	5.22	7.80	10.92	14.04	16.77
HPC	D. Energy	5.70	9.84	15.62	22.15	26.98
HPC	E. Mixed	6.99	12.27	19.77	28.00	33.24

Table A12. Charging time per charging event and per class for AC, DC, and high-power charging events.

Charging Technology	Class	Percentil 25% [h/CE]	Percentil 50% [h/CE]	Percentil 75% [h/CE]	Percentil 90% [h/CE]	Percentil 95% [h/CE]
AC	A. Free	1.50	2.53	3.81	5.10	5.85
AC	B. Flatrate	2.45	3.91	5.31	6.48	7.23
AC	C. Time	1.08	2.09	3.61	5.10	5.87
AC	D. Energy	1.46	2.44	3.52	4.71	5.49
AC	E. Mixed	1.23	2.16	3.18	4.14	4.89
DC	A. Free	0.33	0.59	0.90	1.22	1.41
DC	B. Flatrate	0.70	1.06	1.38	1.56	1.79
DC	C. Time	0.30	0.50	0.85	1.28	1.50
DC	D. Energy	0.36	0.63	1.02	1.36	1.58
DC	E. Mixed	0.36	0.60	0.99	1.37	1.59

Table A12. *Cont.*

Charging Technology	Class	Percentil 25% [h/CE]	Percentil 50% [h/CE]	Percentil 75% [h/CE]	Percentil 90% [h/CE]	Percentil 95% [h/CE]
HPC	A. Free	0.04	0.34	0.60	0.78	0.92
HPC	B. Flatrate	0.50	0.68	0.88	1.08	1.21
HPC	C. Time	0.25	0.36	0.51	0.65	0.76
HPC	D. Energy	0.29	0.47	0.68	0.91	1.07
HPC	E. Mixed	0.31	0.49	0.72	0.96	1.11

Table A13. Idle time per charging event and per class for AC, DC, and high-power charging events.

Charging Technology	Class	Percentil 25% [h/CE]	Percentil 50% [h/CE]	Percentil 75% [h/CE]	Percentil 90% [h/CE]	Percentil 95% [h/CE]
AC	A. Free	0.20	1.09	4.29	8.45	11.27
AC	B. Flatrate	0.26	0.99	4.61	8.33	10.70
AC	C. Time	0.01	0.11	0.86	5.42	6.61
AC	D. Energy	0.12	0.81	3.25	8.55	10.64
AC	E. Mixed	0.03	0.19	0.57	3.40	6.83
DC	A. Free	0	0	0.01	0.04	0.10
DC	B. Flatrate	0	0.03	0.07	0.26	0.72
DC	C. Time	0	0	0.03	0.16	0.48
DC	D. Energy	0	0.01	0.06	0.32	0.79
DC	E. Mixed	0	0	0.02	0.12	0.23
HPC	A. Free	0	0	0.01	0.06	0.11
HPC	B. Flatrate	0	0	0.01	0.02	0.05
HPC	C. Time	0	0	0	0	0
HPC	D. Energy	0	0	0.01	0.05	0.09
HPC	E. Mixed	0	0	0	0.02	0.05

Table A14. Correlation analysis per class for AC, DC, and high-power charging events.

Var. 1	Var. 2	AC Correlation	AC *p*-Value	DC Correlation	DC *p*-Value	HPC Correlation	HPC *p*-Value
A. Free	Duration	0.0451	0	−0.0505	1.4×10^{-65}	−0.0148	1.4×10^{-6}
B. Flatrate	Duration	0.0588	0	0.0595	2.3×10^{-90}	0.1044	8.0×10^{-252}
C. Time	Duration	−0.0546	0	0.0053	7.0×10^{-2}	−0.1229	0
D. Energy	Duration	0.0774	0	0.0288	1.5×10^{-22}	0.0204	3.7×10^{-11}
E. Mixed	Duration	−0.1207	0	−0.0432	1.5×10^{-48}	0.0237	1.5×10^{-14}
A. Free	Energy	0.0153	1.3×10^{-120}	−0.0443	5.5×10^{-51}	−0.0536	1.6×10^{-67}
B. Flatrate	Energy	0.1715	0	0.2735	0	0.2555	0
C. Time	Energy	0.1096	0	−0.1025	3.5×10^{-265}	0.1003	1.9×10^{-232}
D. Energy	Energy	−0.0922	0	−0.0258	2.2×10^{-18}	−0.1403	0
E. Mixed	Energy	−0.0479	0	−0.0242	2.0×10^{-16}	−0.0595	8.5×10^{-83}
A. Free	Avg. Power	−0.0334	0	−0.0042	1.5×10^{-1}	−0.0474	3.1×10^{-53}
B. Flatrate	Avg. Power	0.0359	0	0.0984	3.0×10^{-244}	0.0683	8.9×10^{-109}
C. Time	Avg. Power	0.2095	0	−0.0711	2.1×10^{-128}	0.3619	0
D. Energy	Avg. Power	−0.1550	0	−0.0151	3.0×10^{-7}	−0.1824	0
E. Mixed	Avg. Power	0.0554	0	0.0219	1.0×10^{-13}	−0.1280	0
A. Free	Charge Time	0.0314	0	−0.0530	4.0×10^{-72}	−0.0343	9.7×10^{-29}
B. Flatrate	Charge Time	0.1299	0	0.1896	0	0.1628	0
C. Time	Charge Time	−0.0145	1.2×10^{-108}	−0.0814	1.1×10^{-167}	−0.1816	0
D. Energy	Charge Time	−0.0009	1.6×10^{-1}	−0.0020	4.8×10^{-1}	0.0110	3.3×10^{-4}
E. Mixed	Charge Time	−0.0682	0	−0.0093	1.5×10^{-3}	0.0554	4.0×10^{-72}

Table A14. *Cont.*

Var. 1	Var. 2	AC Correlation	AC *p*-Value	DC Correlation	DC *p*-Value	HPC Correlation	HPC *p*-Value
A. Free	Idle Time	0.0396	0	−0.0389	1.0×10^{-39}	0.0098	1.4×10^{-3}
B. Flatrate	Idle Time	0.0218	5.9×10^{-242}	0.0097	1.0×10^{-3}	−0.0003	9.0×10^{-1}
C. Time	Idle Time	−0.0558	0	0.0289	1.2×10^{-22}	−0.0084	6.1×10^{-3}
D. Energy	Idle Time	0.0864	0	0.0315	1.5×10^{-26}	0.0182	3.6×10^{-9}
E. Mixed	Idle Time	−0.1114	0	−0.0436	2.1×10^{-49}	−0.0163	1.2×10^{-7}

Table A15. Mann–Whitney-U analysis per class for AC charging events.

Class 1	Class 2	Duration s-Value	Duration *p*-Value	Energy s-Value	Energy *p*-Value
A. Free	B. Flatrate	5.10×10^{9}	0	3.40×10^{9}	0
A. Free	C. Time	2.16×10^{10}	0	1.43×10^{10}	0
A. Free	D. Energy	1.67×10^{11}	0	1.66×10^{11}	0
A. Free	E. Mixed	4.52×10^{10}	0	3.88×10^{10}	0
B. Flatrate	A. Free	7.24×10^{9}	0	8.94×10^{9}	0
B. Flatrate	C. Time	8.27×10^{9}	0	7.58×10^{9}	0
B. Flatrate	D. Energy	6.52×10^{10}	0	7.89×10^{10}	0
B. Flatrate	E. Mixed	1.74×10^{10}	0	1.82×10^{10}	0
C. Time	A. Free	1.36×10^{10}	0	2.09×10^{10}	0
C. Time	B. Flatrate	3.51×10^{9}	0	4.20×10^{9}	0
C. Time	D. Energy	1.24×10^{11}	0	1.87×10^{11}	0
C. Time	E. Mixed	3.42×10^{10}	9.07×10^{-7}	4.34×10^{10}	0
D. Energy	A. Free	1.46×10^{11}	0	1.46×10^{11}	0
D. Energy	B. Flatrate	3.95×10^{10}	0	2.58×10^{10}	0
D. Energy	C. Time	1.74×10^{11}	0	1.11×10^{11}	0
D. Energy	E. Mixed	3.62×10^{11}	0	3.09×10^{11}	5.81×10^{-135}
E. Mixed	A. Free	2.60×10^{10}	0	3.24×10^{10}	0
E. Mixed	B. Flatrate	6.38×10^{9}	0	5.58×10^{9}	0
E. Mixed	C. Time	3.36×10^{10}	9.07×10^{-7}	2.44×10^{10}	0
E. Mixed	D. Energy	2.41×10^{11}	0	2.94×10^{11}	5.81×10^{-135}

Table A16. Mann–Whitney-U analysis per class for DC charging events.

Class 1	Class 2	Duration s-Value	Duration *p*-Value	Energy s-Value	Energy *p*-Value
A. Free	B. Flatrate	3.60×10^{7}	0	3.38×10^{7}	0
A. Free	C. Time	1.20×10^{8}	7.90×10^{-7}	1.24×10^{8}	9.58×10^{-23}
A. Free	D. Energy	3.45×10^{8}	1.54×10^{-59}	3.57×10^{8}	3.63×10^{-26}
A. Free	E. Mixed	1.48×10^{8}	1.25×10^{-15}	1.48×10^{8}	2.06×10^{-15}
B. Flatrate	A. Free	9.69×10^{7}	0	9.91×10^{7}	0
B. Flatrate	C. Time	1.35×10^{8}	0	1.45×10^{8}	0
B. Flatrate	D. Energy	4.06×10^{8}	0	4.40×10^{8}	0
B. Flatrate	E. Mixed	1.76×10^{8}	0	1.85×10^{8}	0
C. Time	A. Free	1.13×10^{8}	7.90×10^{-7}	1.09×10^{8}	9.58×10^{-23}
C. Time	B. Flatrate	5.20×10^{7}	0	4.24×10^{7}	0
C. Time	D. Energy	4.73×10^{8}	2.04×10^{-119}	4.66×10^{8}	1.05×10^{-146}
C. Time	E. Mixed	2.02×10^{8}	8.30×10^{-45}	1.93×10^{8}	3.94×10^{-100}
D. Energy	A. Free	4.14×10^{8}	1.54×10^{-59}	4.02×10^{8}	3.63×10^{-26}
D. Energy	B. Flatrate	2.02×10^{8}	0	1.68×10^{8}	0
D. Energy	C. Time	5.94×10^{8}	2.04×10^{-119}	6.01×10^{8}	1.05×10^{-146}
D. Energy	E. Mixed	7.46×10^{8}	6.57×10^{-22}	7.24×10^{8}	1.05×10^{-2}

Table A16. *Cont.*

| Class 1	Class 2	Duration s-Value	Duration *p*-Value	Energy s-Value	Energy *p*-Value
E. Mixed	A. Free	1.64×10^8	1.25×10^{-15}	1.64×10^8	2.06×10^{-15}
E. Mixed	B. Flatrate	7.49×10^7	0	6.61×10^7	0
E. Mixed	C. Time	2.37×10^8	8.30×10^{-45}	2.46×10^8	3.94×10^{-100}
E. Mixed	D. Energy	6.85×10^8	6.57×10^{-22}	7.07×10^8	1.05×10^{-2}

Table A17. Mann–Whitney-U analysis per class for high-power charging events.

| Class 1	Class 2	Duration s-Value	Duration *p*-Value	Energy s-Value	Energy *p*-Value
A. Free	B. Flatrate	9.32×10^5	3.25×10^{-94}	4.80×10^5	3.82×10^{-195}
A. Free	C. Time	4.37×10^6	4.14×10^{-2}	2.03×10^6	1.14×10^{-113}
A. Free	D. Energy	1.37×10^7	3.31×10^{-27}	1.09×10^7	2.07×10^{-65}
A. Free	E. Mixed	4.71×10^6	4.83×10^{-32}	3.87×10^6	4.09×10^{-64}
B. Flatrate	A. Free	2.95×10^6	3.25×10^{-94}	3.41×10^6	3.82×10^{-195}
B. Flatrate	C. Time	9.09×10^7	0	7.70×10^7	0
B. Flatrate	D. Energy	3.03×10^8	0	3.51×10^8	0
B. Flatrate	E. Mixed	1.05×10^8	0	1.24×10^8	0
C. Time	A. Free	4.84×10^6	4.14×10^{-2}	7.18×10^6	1.14×10^{-113}
C. Time	B. Flatrate	2.12×10^7	0	3.51×10^7	0
C. Time	D. Energy	3.88×10^8	0	6.61×10^8	0
C. Time	E. Mixed	1.31×10^8	0	2.34×10^8	0
D. Energy	A. Free	2.35×10^7	3.31×10^{-27}	2.64×10^7	2.07×10^{-65}
D. Energy	B. Flatrate	1.50×10^8	0	1.02×10^8	0
D. Energy	C. Time	6.86×10^8	0	4.13×10^8	0
D. Energy	E. Mixed	7.46×10^8	8.19×10^{-15}	7.70×10^8	0.53
E. Mixed	A. Free	8.55×10^6	4.83×10^{-32}	9.38×10^6	4.09×10^{-64}
E. Mixed	B. Flatrate	5.61×10^7	0	3.71×10^7	0
E. Mixed	C. Time	2.51×10^8	0	1.48×10^8	0
E. Mixed	D. Energy	7.99×10^8	8.19×10^{-15}	7.75×10^8	0.53
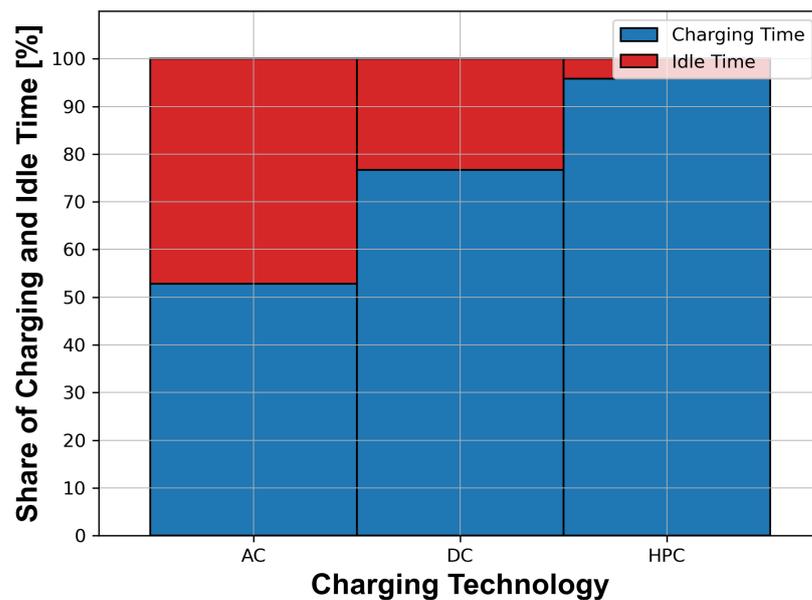
(**a**) Share of charging and idle time

Figure A16. *Cont.*
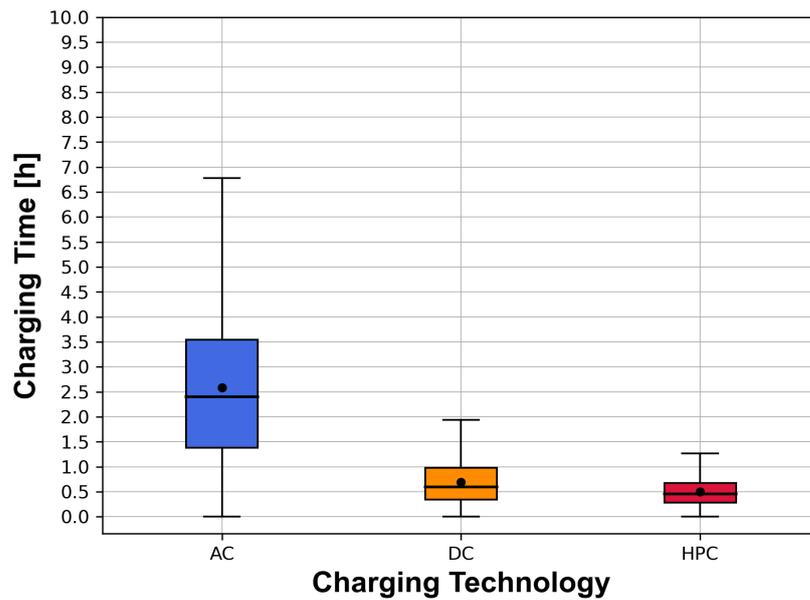
(**b**) Charging Time

Figure A16. Charging and idle time of AC, DC and high-power charging events.
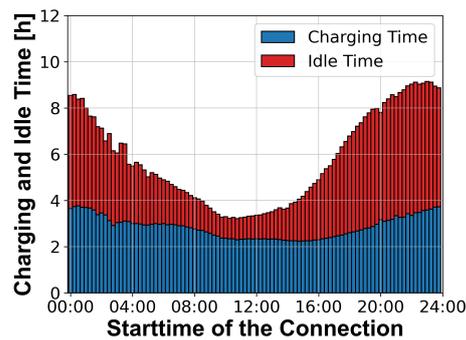
(**a**) AC charging events
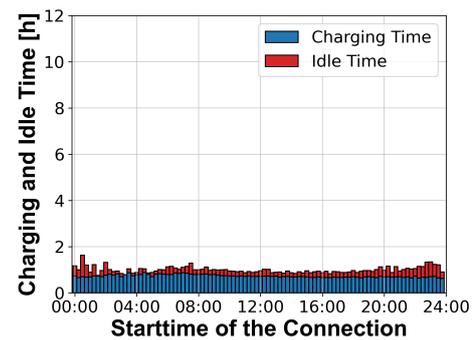
(**b**) DC charging events
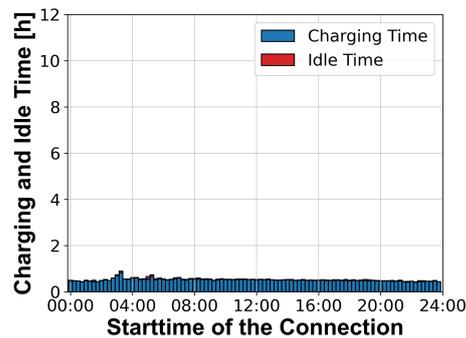
(**c**) High-power charging events

Figure A17. Average charging and idle time of AC, DC, and high-power charging events depending on the connection start time.

References

1. Bleviss, D.L. Transportation is critical to reducing greenhouse gas emissions in the United States. *WIREs Energy Environ.* **2021**, *10*, e390. [CrossRef]
2. Mogoș, R.I.; Petrescu, I.; Chiotan, R.A.; Crețu, R.C.; Troacă, V.A.; Mogoș, P.L. Greenhouse gas emissions and Green Deal in the European Union. *Front. Environ. Sci.* **2023**, *11*, 1141473. [CrossRef]

3. Greenhouse Gas Emissions. *Total U.S. Greenhouse Gas Emissions by Economic Sector in 2021*; United States Environmental Protection Agency: Washington, DC, USA, 2021.
4. Transport and Mobility. 2024. Available online: https://www.eea.europa.eu/en/topics/in-depth/transport-and-mobility?activeTab=fa515f0c-9ab0-493c-b4cd-58a32dfaae0a (accessed on 17 April 2024).
5. Publications Office of the European Union. *EU Transport in Figures: Statistical Pocketbook*; Publications Office of the European Union: Luxembourg, 2022; Volume 2022.
6. United States Environmental Protection Agency. U.S. Transportation Sector Greenhouse Gas Emissions 1990–2021. 2023. Available online: https://www.epa.gov/system/files/documents/2023-06/420f23016.pdf (accessed on 17 April 2024).
7. Irle, R. Global EV Sales for 2023. 2024. Available online: https://ev-volumes.com/news/ev/global-ev-sales-for-2023/ (accessed on 17 April 2024).
8. Irle, R. Global EV Sales for 2022. 2023. Available online: https://ev-volumes.com/news/ev/global-ev-sales-for-2022/ (accessed on 17 April 2024).
9. Rostad Sæther, S. Mobility at the crossroads—Electric mobility policy and charging infrastructure lessons from across Europe. *Transp. Res. Part Policy Pract.* **2022**, *157*, 144–159. [CrossRef]
10. Haidar, B.; Aguilar Rojas, M.T. The relationship between public charging infrastructure deployment and other socio-economic factors and electric vehicle adoption in France. *Res. Transp. Econ.* **2022**, *95*, 101208. [CrossRef]
11. Luo, Q.; Yin, Y.; Chen, P.; Zhan, Z.; Saigal, R. Dynamic subsidies for synergistic development of charging infrastructure and electric vehicle adoption. *Transp. Policy* **2022**, *129*, 117–136. [CrossRef]
12. Shoup, D.C. The High Cost of Free Parking. *J. Plan. Educ. Res.* **1997**, *17*, 3–20. [CrossRef]
13. Litman, T. *Parking Management Best Practices*; Routledge: New York, NY, USA, 2005.
14. Ottosson, D.B.; Chen, C.; Wang, T.; Lin, H. The sensitivity of on-street parking demand in response to price changes: A case study in Seattle, WA. *Transp. Policy* **2013**, *25*, 222–232. [CrossRef]
15. Sun, X.H.; Yamamoto, T.; Morikawa, T. Charge timing choice behavior of battery electric vehicle users. *Transp. Res. Part Transp. Environ.* **2015**, *37*, 97–107. [CrossRef]
16. Sun, X.H.; Yamamoto, T.; Morikawa, T. Stochastic frontier analysis of excess access to mid-trip battery electric vehicle fast charging. *Transp. Res. Part Transp. Environ.* **2015**, *34*, 83–94. [CrossRef]
17. van den Hoed, R.; Helmus, J.R.; de Vries, R.; Bardok, D. Data analysis on the public charge infrastructure in the city of Amsterdam. In Proceedings of the 2013 World Electric Vehicle Symposium and Exhibition (EVS27), Barcelona, Spain, 17–20 November 2013; IEEE: Piscataway, NJ, USA, 2013; pp. 1–10. [CrossRef]
18. Motoaki, Y.; Shirk, M.G. Consumer behavioral adaption in EV fast charging through pricing. *Energy Policy* **2017**, *108*, 178–183. [CrossRef]
19. Morrissey, P.; Weldon, P.; O'Mahony, M. Future standard and fast charging infrastructure planning: An analysis of electric vehicle charging behaviour. *Energy Policy* **2016**, *89*, 257–270. [CrossRef]
20. Wolbertus, R.; van den Hoed, R.; Maase, S. Benchmarking Charging Infrastructure Utilization. *World Electr. Veh. J.* **2016**, *8*, 754–771. [CrossRef]
21. Wolbertus, R.; van den Hoed, R. Charging Station Hogging: A Data-Driven Analysis. In Proceedings of the Electric Vehicle Symposium EVS30, Stuttgart, Germany, 9–11 October 2017.
22. van der Kam, M.; van Sark, W.; Alkemade, F. Multiple roads ahead: How charging behavior can guide charging infrastructure roll-out policy. *Transp. Res. Part Transp. Environ.* **2020**, *85*, 102452. [CrossRef]
23. Wolbertus, R.; Van den Hoed, R.; Kroesen, M.; Chorus, C. Charging infrastructure roll-out strategies for large scale introduction of electric vehicles in urban areas: An agent-based simulation study. *Transp. Res. Part Policy Pract.* **2021**, *148*, 262–285. [CrossRef]
24. Fischer, M.; Hardt, C.; Michalk, W.; Bogenberger, K. Charging or Idling: Method for quantifying the Charging and the Idle Time of public Charging Stations. In *Proceedings of the TRB 101st Annual Meeting Compendium of Papers*; Transportation Research Board: Washington, DC, USA, 2022; p. 22.
25. Hecht, C.; Das, S.; Bussar, C.; Sauer, D.U. Representative, empirical, real-world charging station usage characteristics and data in Germany. *eTransportation* **2020**, *6*, 100079. [CrossRef]
26. Friese, P.A.; Michalk, W.; Fischer, M.; Hardt, C.; Bogenberger, K. Charging Point Usage in Germany—Automated Retrieval, Analysis, and Usage Types Explained. *Sustainability* **2021**, *13*, 13046. [CrossRef]
27. Mortimer, B.J.; Hecht, C.; Goldbeck, R.; Sauer, D.U.; de Doncker, R.W. Electric Vehicle Public Charging Infrastructure Planning Using Real-World Charging Data. *World Electr. Veh. J.* **2022**, *13*, 94. [CrossRef]
28. Hecht, C.; Figgener, J.; Sauer, D.U. Analysis of Electric Vehicle Charging Station Usage and Profitability in Germany based on Empirical Data. *arXiv* **2022**, arXiv:2206.09582. [CrossRef]
29. Jonas, T.; Daniels, N.; Macht, G. Electric Vehicle User Behavior: An Analysis of Charging Station Utilization in Canada. *Energies* **2023**, *16*, 1592. [CrossRef]
30. Borlaug, B.; Yang, F.; Pritchard, E.; Wood, E.; Gonder, J. Public electric vehicle charging station utilization in the United States. *Transp. Res. Part Transp. Environ.* **2023**, *114*, 103564. [CrossRef]
31. Mahlberg, J.A.; Desai, J.; Bullock, D.M. Evaluation of Electric Vehicle Charging Usage and Driver Activity. *World Electr. Veh. J.* **2023**, *14*, 308. [CrossRef]
32. *DIN SPEC 91412*; Electric Mobility Terminology and Graphical Symbols. Beuth Publishing DIN: Berlin, Germany, 2020.

33. BDEW Bundesverband der Energie- und Wasserwirtschaft e.V. Elektromobilität Definition der Ladeinfrastruktur-Marktrollen. 2020. Available online: https://www.bdew.de/media/documents/201008_PG-LIS_Definitionen_Marktrollen_neu.pdf (accessed on 17 April 2024).

34. King, C.; Datta, B. EV charging tariffs that work for EV owners, utilities and society. *Electr. J.* **2018**, *31*, 24–27. [CrossRef]

35. Fischer, M.; Hardt, C.; Elias, J.; Bogenberger, K. Simulation-Based Evaluation of Charging Infrastructure Concepts: The Park and Ride Case. *World Electr. Veh. J.* **2022**, *13*, 151. [CrossRef]

36. Aisbl, E. EuroGlobalMap, Topographic Dataset Covering 55 Countries and Territories in the European Region. 2023. Available online: https://www.mapsforeurope.org/datasets/euro-global-map (accessed on 17 April 2024).

37. Eurostat. NUTS—Nomenclature of Territorial Units for Statistics: Urban-Rural Typology. 2023. Available online: https://ec.europa.eu/eurostat/statistics-explained/index.php?title=Glossary:Urban-rural_typology (accessed on 17 April 2024).

38. European Parliament, Council of the European Union. Directive 2014/94/EU of the European Parliament and of the Council of 22 October 2014 on the deployment of alternative fuels infrastructure Text with EEA relevance. *Off. J. Eur. Union* **2014**, *307*, 1–20.

39. *BGBl. I S. 457*; Verordnung über Technische Mindestanforderungen an Den Sicheren und Interoperablen Aufbau und Betrieb von öffentlich Zugänglichen Ladepunkten Für Elektrisch Betriebene Fahrzeuge[1] (Ladesäulenverordnung—LSV). Bundesministerium der Justiz (BMJ): Berlin, Germany, 2023.

40. Rechtsgutachten zur Anwendbarkeit von § 3 Preisangabenverordnung (PAngV) auf Ladestrom für Elektromobile Sowie zur Zulässigkeit und Vereinbarkeit verschiedener am Markt Befindlicher Tarifmodelle für Ladestrom Mit den Vorgaben der PAngV. 2018. Available online: https://www.bmwk.de/Redaktion/DE/Downloads/P-R/preisangabe-fuer-und-abrechnung-von-ladestrom-fuer-elektromobile-rechtsgutachten.pdf?__blob=publicationFile&v=10 (accessed on 17 April 2024).

41. Ministère de L'environnement, de L'énergie et de la mer, en Charge des Relations Internationales sur le Climat. Décret no 2017-26 du 12 janvier 2017 relatif aux infrastructures de recharge pour véhicules électriques et portant diverses mesures de transposition de la directive 2014/94/UE du Parlement européen et du Conseil du 22 octobre 2014 sur le déploiement d'une infrastructure pour carburants alternatifs. *J. Off. Républ. Fr.* **2017**. Available online: https://www.legifrance.gouv.fr/download/pdf?id=s5eqBcWZrBzfgEUbcYcs7q38cKGNTdip-H2yghvSZQU= (accessed on 17 April 2024).

42. Schuster, A. Batterie-bzw. Wasserstoffspeicher Bei Elektrischen Fahrzeugen. Ph.D. Thesis, Technical University of Vienna, Vienna, Austria, 2008.

43. Lima, P. Samsung SDI 94 Ah Battery Cell Full Specifications. *PushEVs*, 2021. Available online: https://pushevs.com/2018/04/05/samsung-sdi-94-ah-battery-cell-full-specifications (accessed on 17 April 2024).

44. Kruskal, W.H.; Wallis, W.A. Use of Ranks in One-Criterion Variance Analysis. *J. Am. Stat. Assoc.* **1952**, *47*, 583. [CrossRef]

45. Mann, H.B.; Whitney, D.R. On a Test of Whether one of Two Random Variables is Stochastically Larger than the Other. *Ann. Math. Stat.* **1947**, *18*, 50–60. [CrossRef]

46. Tate, R.F. Correlation Between a Discrete and a Continuous Variable. Point-Biserial Correlation. *Ann. Math. Stat.* **1954**, *25*, 603–607.

47. Johnsen, D.; Ostendorf, L.; Bechberger, M.; Strommenger, D. Review on Smart Charging of Electric Vehicles via Market-Based Incentives, Grid-Friendly and Grid-Compatible Measures. *World Electr. Veh. J.* **2023**, *14*, 25. [CrossRef]

48. Wolbertus, R.; Heath, E.; Heller, R. Impact of battery developments on the future of charging infrastructure deployment. In Proceedings of the Electric Vehicle Symposium 35, Oslo, Norway, 11–15 June 2022.

49. Lee, Z.J.; Pang, J.Z.; Low, S.H. Pricing EV charging service with demand charge. *Electr. Power Syst. Res.* **2020**, *189*, 106694. [CrossRef]

50. Rancilio, G.; Bovera, F.; Delfanti, M. Tariff–based regulatory sandboxes for EV smart charging: Impacts on the tariff and the power system in a national framework. *Int. J. Energy Res.* **2022**, *46*, 14794–14813. [CrossRef]